AFRL-ML-WP-TR-2003-4036

JOINING OF GAMMA TITANIUM ALUMINIDES

LTC William A. Baeslack, III

Metals Branch (AFRL/MLLM)
Metals, Ceramics, and NDE Division
Materials and Manufacturing Directorate
Air Force Research Laboratory, Air Force Materiel Command
Wright-Patterson Air Force Base, OH 45433-7750

SEPTEMBER 2002

Final Report for 01 November 1999 – 01 September 2002

Approved for public release; distribution is unlimited.

MATERIALS AND MANUFACTURING DIRECTORATE
AIR FORCE RESEARCH LABORATORY
AIR FORCE MATERIEL COMMAND
WRIGHT-PATTERSON AIR FORCE BASE, OH 45433-7750

NOTICE

WHEN GOVERNMENT DRAWINGS, SPECIFICATIONS, OR OTHER DATA ARE USED FOR ANY PURPOSE OTHER THAN IN CONNECTION WITH A DEFINITELY GOVERNMENT-RELATED PROCUREMENT, THE UNITED STATES GOVERNMENT INCURS NO RESPONSIBILITY OR ANY OBLIGATION WHATSOEVER. THE FACT THAT THE GOVERNMENT MAY HAVE FORMULATED OR IN ANY WAY SUPPLIED THE SAID DRAWINGS, SPECIFICATIONS, OR OTHER DATA, IS NOT TO BE REGARDED BY IMPLICATION OR OTHERWISE IN ANY MANNER CONSTRUED, AS LICENSING THE HOLDER OR ANY OTHER PERSON OR CORPORATION, OR AS CONVEYING ANY RIGHTS OR PERMISSION TO MANUFACTURE, USE, OR SELL ANY PATENTED INVENTION THAT MAY IN ANY WAY BE RELATED THERETO.

THIS REPORT IS RELEASABLE TO THE NATIONAL TECHNICAL INFORMATION SERVICE (NTIS). AT NTIS, IT WILL BE AVAILABLE TO THE GENERAL PUBLIC, INCLUDING FOREIGN NATIONS.

THIS TECHNICAL REPORT HAS BEEN REVIEWED AND IS APPROVED FOR PUBLICATION.

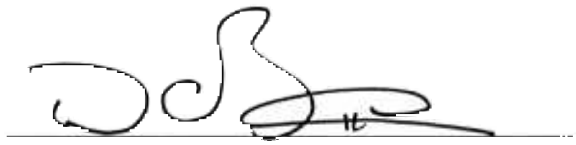

DR. WILLIAM A. BAESLACK, LT COL
Metals Branch
Metals, Ceramics & NDE Division

DR. ROLLIE E. DUTTON, Chief
Metals Branch
Metals, Ceramics & NDE Division

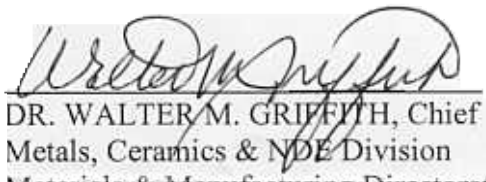

DR. WALTER M. GRIFFITH, Chief
Metals, Ceramics & NDE Division
Materials & Manufacturing Directorate

IF YOUR ADDRESS HAS CHANGED, IF YOU WISH TO BE REMOVED FROM OUR MAILING LIST, OR IF THE ADDRESSEE IS NO LONGER EMPLOYED BY YOUR ORGANIZATION, PLEASE NOTIFY, AFRL/MLLMD, WRIGHT-PATTERSON AFB OH 45433-7817 TO HELP US MAINTAIN A CURRENT MAILING LIST.

COPIES OF THIS REPORT SHOULD NOT BE RETURNED UNLESS RETURN IS REQUIRED BY SECURITY CONSIDERATIONS, CONTRACTUAL OBLIGATIONS, OR NOTICE ON A SPECIFIC DOCUMENT.

REPORT DOCUMENTATION PAGE

Form Approved
OMB No. 0704-0188

The public reporting burden for this collection of information is estimated to average 1 hour per response, including the time for reviewing instructions, searching existing data sources, searching existing data sources, gathering and maintaining the data needed, and completing and reviewing the collection of information. Send comments regarding this burden estimate or any other aspect of this collection of information, including suggestions for reducing this burden, to Department of Defense, Washington Headquarters Services, Directorate for Information Operations and Reports (0704-0188), 1215 Jefferson Davis Highway, Suite 1204, Arlington, VA 22202-4302. Respondents should be aware that notwithstanding any other provision of law, no person shall be subject to any penalty for failing to comply with a collection of information if it does not display a currently valid OMB control number. **PLEASE DO NOT RETURN YOUR FORM TO THE ABOVE ADDRESS**.

1. REPORT DATE *(DD-MM-YY)*	2. REPORT TYPE	3. DATES COVERED *(From - To)*
September 2002	Final	11/01/1999 – 09/01/2002

4. TITLE AND SUBTITLE
JOINING OF GAMMA TITANIUM ALUMINIDES

5a. CONTRACT NUMBER
In-house

5b. GRANT NUMBER

5c. PROGRAM ELEMENT NUMBER
62102F

6. AUTHOR(S)
LTC William A. Baeslack, III

5d. PROJECT NUMBER
MO2R

5e. TASK NUMBER
10

5f. WORK UNIT NUMBER
00

7. PERFORMING ORGANIZATION NAME(S) AND ADDRESS(ES)

Metals Branch (AFRL/MLLM)
Metals, Ceramics, and NDE Division
Materials and Manufacturing Directorate
Air Force Research Laboratory, Air Force Materiel Command
Wright-Patterson Air Force Base, OH 45433-7750

8. PERFORMING ORGANIZATION REPORT NUMBER

9. SPONSORING/MONITORING AGENCY NAME(S) AND ADDRESS(ES)
Materials and Manufacturing Directorate
Air Force Research Laboratory
Air Force Materiel Command
Wright-Patterson AFB, OH 45433-7750

10. SPONSORING/MONITORING AGENCY ACRONYM(S)
AFRL/MLLM

11. SPONSORING/MONITORING AGENCY REPORT NUMBER(S)
AFRL-ML-WP-TR-2003-4036

12. DISTRIBUTION/AVAILABILITY STATEMENT
Approved for public release; distribution is unlimited.

13. SUPPLEMENTARY NOTES
Report contains color.

14. ABSTRACT

This report summarizes, interprets and comparatively discusses the results of research and development performed on the joining of gamma titanium aluminides during the past two decades. Although organized and presented by joining process, many of the observations made and relationships developed, particularly those regarding the weldability and welding metallurgy of gamma titanium aluminides, are broadly applicable. Generally, the basic welding processes and techniques utilized in the fusion and solid-state friction welding of conventional titanium alloys can also be applied to the welding of gamma titanium aluminides. However, the welding process parameters must be optimized, and in some instances the welding system significantly modified, to provide a comparatively slow weld cooling rate that minimizes the potential for solid-state weld cracking, and that promotes the formation of a weld zone microstructure that exhibits suitable mechanical properties. Control of the weld cooling rate and the application of a postweld heat treatment can be used to generate a wide range of crack-free weld zone microstructures that correspondingly offer a range of mechanical property combinations. Gamma titanium aluminides can also be effectively joined using diffusion welding and conventional and diffusion brazing techniques.

15. SUBJECT TERMS
gamma titanium aluminide, joining, welding, weldability, gas tungsten-arc welding, laser welding, electron beam welding, friction welding, diffusion welding, brazing, solidification, phase transformations, mechanical properties, fracture behavior

16. SECURITY CLASSIFICATION OF:			17. LIMITATION OF ABSTRACT:	18. NUMBER OF PAGES	19a. NAME OF RESPONSIBLE PERSON (Monitor)
a. REPORT	b. ABSTRACT	c. THIS PAGE			Rollie Dutton
Unclassified	Unclassified	Unclassified	SAR	118	19b. TELEPHONE NUMBER *(Include Area Code)* (937) 255-1305

Standard Form 298 (Rev. 8-98)
Prescribed by ANSI Std. Z39-18

TABLE OF CONTENTS

LIST OF FIGURES

ACKNOWLEDGEMENTS

The author would like to acknowledge the contributions of many students at The Ohio State University for providing photographs and informa tion presented in this review. The many contributions of Mr. Tom Kelly of GE Aircraft Engines, Cincinnati, Ohio, and Dr. P. L. Threadgill of TWI to the work described in this document are also very much appreciated.

EXECUTIVE SUMMARY

This report summarizes, interprets and comparatively discusses the results of research and development performed on the joining of gamma titanium aluminides during the past two decades. Although organized and presented by joining process, many of the observations made and relationships developed, particularly those regarding the weldability and welding metallurgy of gamma titanium aluminides, are broadly applicable.

Generally, the basic welding processes and techniques utilized in the fusion and solid-state friction welding of conventional titanium alloys can also be applied to the welding of gamma titanium aluminides. However, the welding process parameters must be optimized, and in some instances the welding system significantly modified, to provide a comparatively slow weld cooling rate that minimizes the potential for solid-state weld cracking, and that promotes the formation of a weld zone microstructure that exhibits suitable mechanical properties either as-welded or following a suitable postweld heat treatment. Gamma titanium aluminides can also be effectively joined using diffusion welding and conventional and diffusion brazing techniques.

As for conventional titanium alloys, gamma titanium aluminides exhibit low susceptibility to weld solidification or heat-affected-zone liquation cracking during fusion welding. However, as indicated above, they are highly susceptible to solid-state cracking during weld cooling, which has been shown to originate from the combination of a brittle weld zone microstructure and high weld thermal stresses, with possible environmental effects. Several investigators have shown that lowering the weld cooling rate reduces or eliminates susceptibility to solid-state cracking by promoting transformation of the weld

zone to a more crack resistant gamma + alpha-two microstructure, versus rapidly-cooled microstructures that contain retained alpha-two phase, and also by reducing the weld thermal stresses. Preventing the exposure of the as-welded workpiece to the atmosphere prior to postweld stress relief heat treatment also reduces solid-state cracking susceptibility.

Control of the weld cooling rate and the application of a postweld heat treatment can be used to generate a wide range of crack-free weld zone microstructures that correspondingly exhibit a range of mechanical property combinations. Microstructures generated at higher weld cooling rates, comprised of massive or Widmanstatten gamma phase, and/or fine lamellar gamma + alpha-two constituent (or mixtures of these different phases/constituents), are high in strength, but exhibit low ductility and fracture toughness relative to typical equiaxed gamma, duplex, or fully lamellar base metal microstructures. Coarser lamellar gamma + alpha-two microstructures produced at lower weld cooling rates exhibit lower strength (albeit greater than the base metal), marginal ductility, but improved fracture toughness. Postweld heat treatment at temperatures ranging from 1000 to 1250^{o}C can be used to provide stress relief, and to modify (e.g., recrystallization to an equiaxed gamma or duplex microstructure) and stabilize the weld zone microstructure without markedly affecting the base metal microstructure and mechanical properties. The effective control of the weld thermal cycle and subsequent postweld heat treatment can be utilized to generate an optimized combination of mechanical properties in the weld zone.

Although geometry restricted, diffusion welding has been demonstrated to be effective in producing high integrity bonds with minimal change from the base metal, and

no propensity for solid-state cracking. Diffusion brazing techniques, including transient-liquid-phase approaches, have also been demonstrated to be effective for the joining of gamma titanium aluminides, however, the optimization of joint strength and ductility requires a high temperature postbraze diffusion heat treatment to homogenize the significant compositional differences that exist in the as-brazed joint, and thereby achieve acceptable joint mechanical properties. These techniques have also been demonstrated to be more effective than fusion and solid-state friction welding techniques for the dissimilar-alloy joining of gamma titanium aluminides to conventional titanium alloys.

1. INTRODUCTION

During the past decade, gamma titanium aluminides have become recognized as a class of structural intermetallics that offers significant potential for application in advanced aerospace systems and automotive components [1-3]. With a density approximately one-half of Ni-base superalloys and 10% less than conventional titanium alloys, and a utilization temperature of up to 750^{o}C, gamma titanium aluminides offer the potential for significant weight reduction in high-temperature components. During the 1990's tremendous progress was achieved in gamma titanium aluminide alloy development, the processing of both cast and wrought (including powder perform) product forms, and the fabrication and testing of actual full-scale components. At the present time, a wide range of semi-commercial and commercial alloy combinations is available, ranging from GE's broadly-assessed Ti-48Al-2Nb-2Cr (at%) alloy to recently developed, more compositionally complex alloys. These alloys are available in a variety of product forms, ranging from investment castings (typically HIP'ed) to hot-rolled sheet. Extensive processing/heat treatment studies have lead to the availability of a wide range of alloy microstructures that can be tailored to achieve the desired mechanical properties. As a result, mechanical property combinations can now be obtained that are superior to those exhibited by conventional titanium alloys and nickel-base superalloys. Current alloys exhibit a specific elastic modulus that is 50-70% greater than conventional titanium alloys, and elevated-temperature specific strengths superior to conventional titanium alloys and polycrystalline Ni-based superalloys. Oxidation resistance and creep resistance are also excellent, and superior to conventional titanium alloys. Although comparatively low room temperature tensile ductility and fracture toughness limits the

application of these materials in fracture critical applications, they are sufficient to meet many design requirements.

A recent analysis by Dimiduk [1] developed property maps that compare property combinations of intermetallics with conventional structural materials. This analysis revealed new and attractive property balances for gamma titanium aluminides, particularly in the context of the density-normalized properties and high temperature capabilities that will make these materials competitive for many potential applications. Figure 1 shows the superior specific modulus (a) and specific strength (b) characteristics of gamma titanium aluminides relative to several other classes of structural aerospace materials [1].

The broad application of gamma titanium aluminides in structural applications will demand their joining in both original manufacture and repair. Although the joining of gamma titanium aluminides compares well with that of conventional high-strength titanium alloys, particularly from the standpoints of preweld cleaning and atmosphere control requirements, the low toughness and ductility of the base metal and the weld zone can lead to severe solid-state cracking during weld cooling. The avoidance of such cracking, combined with the production of an optimum weld zone microstructure and mechanical properties, typically requires the application of welding processes that have been specially adapted to provide controlled, comparatively slow cooling rates, and postweld heat treatment. Nonetheless, in recent years, a wide range of fusion and solid-state joining processes have been successfully applied to the joining of gamma titanium aluminides.

The joining of gamma titanium aluminides was reviewed by Threadgill [4-6] from TWI in several papers throughout the 1990's. Cam and Kocak [7] also discussed this topic as part of a much broader review of advanced materials. Although very informative, these reports were not fully comprehensive nor do they describe the appreciable work performed on the joining of gamma titanium aluminides during the late 1990's. This review provides an updated and more comprehensive review of this topic. It describes the application of both fusion and solid-state welding and joining techniques to gamma titanium aluminides. The following sections review in detail research and development that has been performed on the joining of gamma titanium aluminides over the past decade using these various joining processes. Although the section is organized and presented by joining process, many of the observations and principles developed, particularly those pertaining to the welding metallurgy of gamma titanium aluminides, are broadly applicable. Relationships between the thermal and mechanical conditions experienced during joining and subsequent postweld heat treatment, and evolution of the resulting joint microstructures, and relationships between these microstructures and the propensity for defect formation, mechanical properties, and fracture behavior, are described with the overall goal of identifying approaches toward optimizing joint performance.

As a precursor to this review and analysis, the following Background section provides a brief overview of joining processes applicable to gamma titanium aluminides, and the solidification and solid-state phase transformation behavior of gamma titanium aluminides.

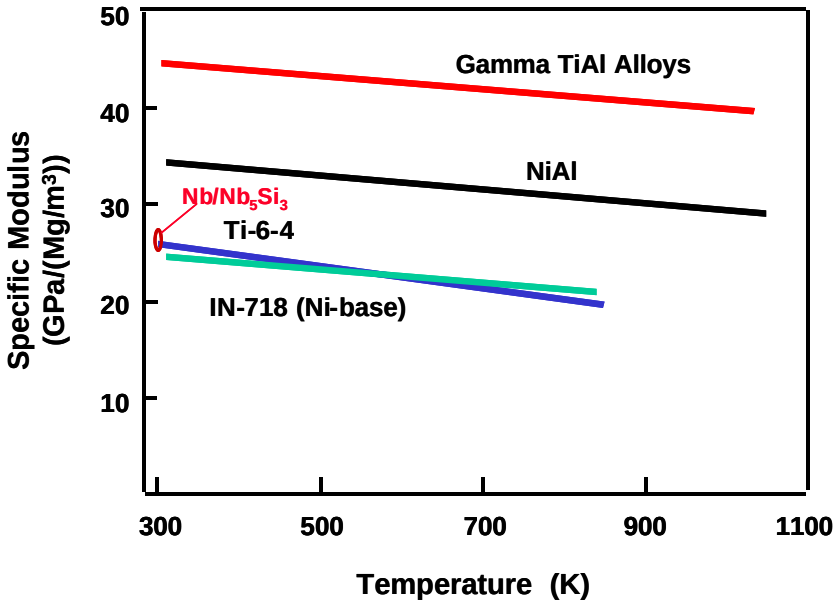

a.

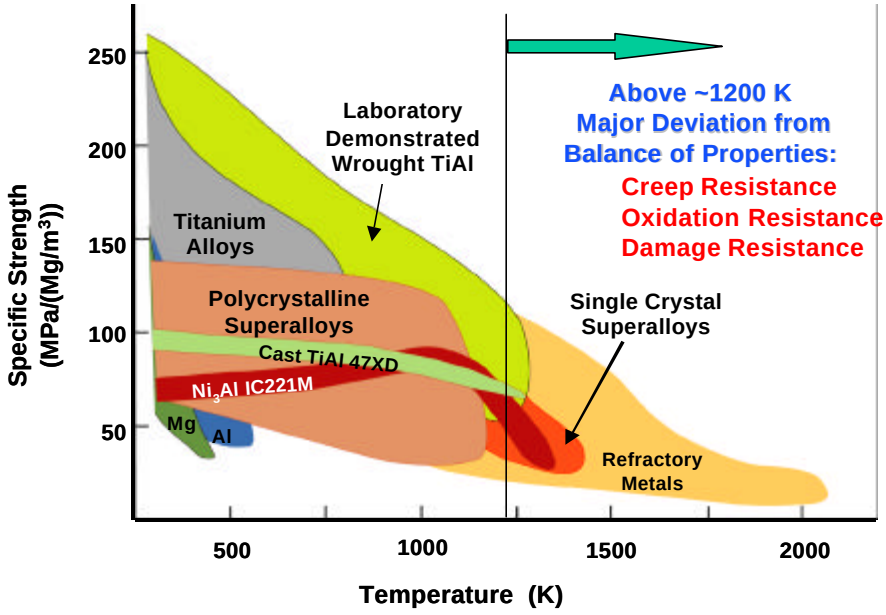

b.

Figure 1. Density normalized or specific properties of structural alloys and selected intermetallics [1]: (a) specific modulus versus temperature; (b) specific strength versus temperature.

3.0 BACKGROUND

3.1 Joining Processes Applicable to Gamma Titanium Aluminides

A wide range of fusion and solid-state welding processes have been utilized to join gamma titanium aluminides. Since this alloy family was originally developed primarily for the manufacture of aerospace propulsion systems, numerous joining processes commonly utilized by the aerospace industry have been applied with varying degrees of success.

A major emphasis on the development and application of investment cast gamma titanium aluminides in the early 1990's stimulated significant work on gas tungsten-arc welding (GTAW) both for the welding of individual castings into built-up structures and for the repair of casting defects. This welding process can be performed manually or automatically, and either autogenously (i.e., no filler metal added) for thin sections or with the addition of a filler metal for thick sections. As with conventional titanium alloys, gamma titanium aluminides must be suitably cleaned prior to welding in order to avoid hydrogen-induced porosity, and completely shielded from atmospheric contamination during and immediately subsequent to welding using an inert-gas environment. Requirements to minimize the weld cooling rate in order to prevent solid-state cracking during weld cooling have typically required process adaptations including the use of welding fixtures and welding parameters that can accurately and reproducibly control comparatively high preheat and interpass temperatures, and the weld cooling rate. Such special fixtures range from relatively simple arrangements using quartz heating lamps, to much more sophisticated and expensive resistance heated fixturing and inert gas shielding systems. Based on evidence that exposure of the as-cooled weld to the

atmosphere can promote solid-state cracking susceptibility due to an environmental effect, some GTAW systems provide for the direct transfer of the welded component from the welding chamber to a vacuum furnace without cooling the specimen to room temperature or exposing it to the atmosphere. Typical preheat and interpass temperatures for the multipass GTAW of gamma plate would be 800°C.

Electron beam welding (EBW) and laser beam welding (LBW), due to their deep penetration capabilities, have also been extensively investigated from both process and metallurgical perspectives. Because of the extremely high heating and cooling rates associated with these high-energy-density heat source, but low net energy input processes, the utilization of preheat and interpass temperature control to reduce weld heating and cooling rates is extremely important. Although this has been accomplished in small specimens by rastering the beam across the joint region to preheat to high temperatures, such an approach is not practical for large-scale welds. Preheating capabilities have been incorporated into large electron beam welding chambers, thereby allowing deep-penetration electron-beam welding combined with relatively slow weld cooling rates to prevent solid-state cracking and promote superior weld zone microstructures and mechanical properties.

A diversity of friction welding processes have been successfully applied for the similar and dissimilar alloy joining of gamma titanium aluminides. These include inertia-friction welding (IFW) and continuous-drive friction welding (CDFW) processes that are widely used to join axially symmetric components, and more recently developed variations of friction welding that can produce joints between plate, sheet and other geometries, such as the linear-friction welding (LFW) and friction-stir welding (FSW)

processes. Cooling rates experienced during the welding of conventional titanium alloys using these processes can be sufficiently high to promote solid-state cracking in gamma titanium aluminides (typically a few hundred ^{o}C/s). Although external heating of friction welds has been used to reduce and control the weld cooling rate, a reduction in cooling rate is generally more easily obtained through process parameter control.

Finally, diffusion welding (DW) (with and without metallic interlayers) and diffusion brazing (including transient liquid phase brazing) have also been evaluated as processes that eliminate cracking problems commonly associated with fusion and friction welding. These processes also offer a strong potential for the dissimilar-alloy welding of gamma titanium aluminides to conventional titanium alloys and other materials. Diffusion welding also has the potential to be combined with superplastic forming in the fabrication of complex components

3.2 Solidification and Solid-State Phase Transformations in Gamma Titanium Aluminides

Solidification behavior and subsequent solid-state phase transformations during continuous cooling determine the characteristics of the as-welded microstructure. These phenomena also influence susceptibility of a weld fusion zone to both solidification and solid-state cracking. As shown in Figure 2 [8], the solidification of Al-rich Ti alloys occurs through a series of cascading peritectics. Although the solidification behavior of cast gamma titanium aluminides has been investigated for both binary [9,10] and more complex alloys [11,12], particularly in the cast form, a comprehensive understanding of compositional, cooling rate and solidification rate effects on the macrosolidification

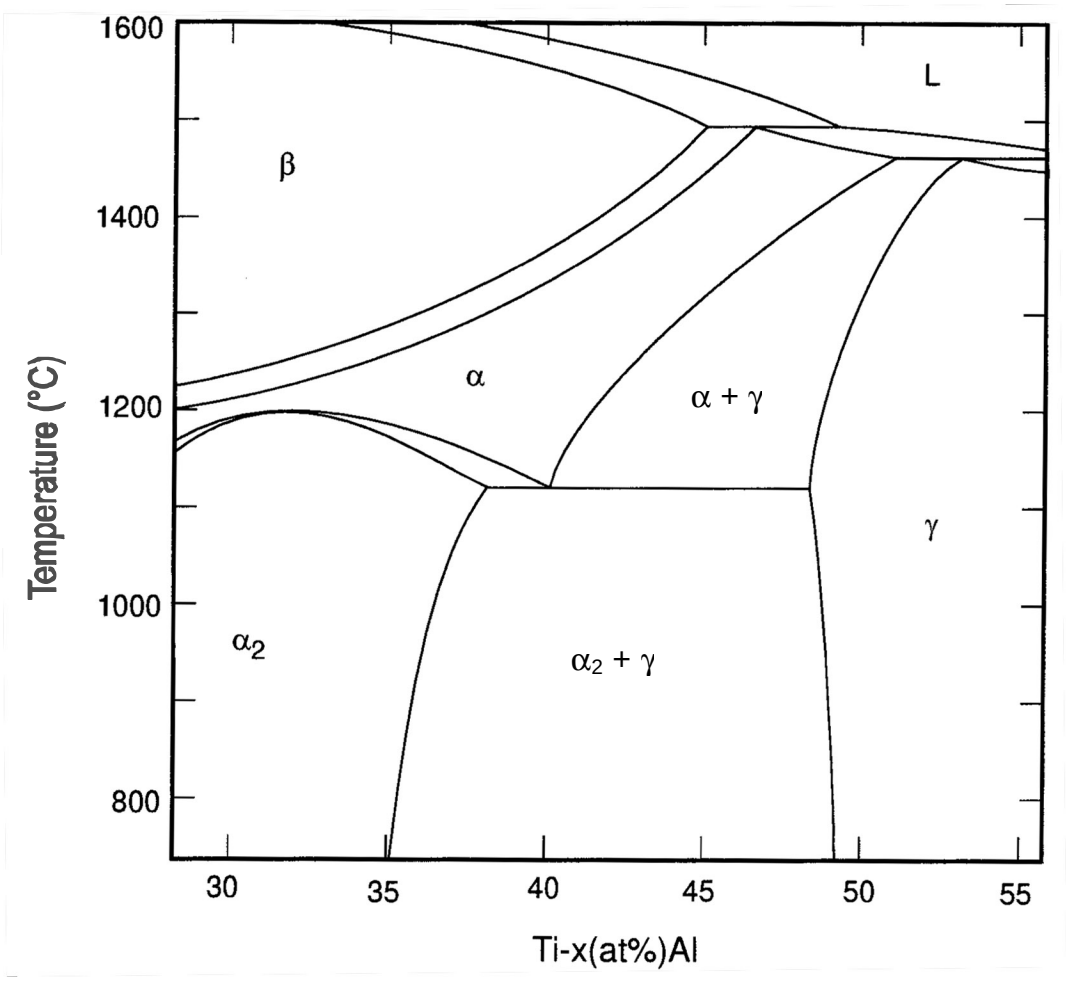

Figure 2. Ti-rich side of the Ti-Al binary phase diagram [8].

characteristics (i.e., grain structure) and the microsolidification characteristics (i.e., phase(s), dendritic structure) does not exist. Early studies by McCullough et al. [9,10] showed the solidification of binary Ti-40-49%Al alloys to occur as primary beta phase, and Ti-49-55%Al alloys to occur as primary alpha phase, with interdendritic gamma segregate observed at Al contents greater than 46% (all compositions are in atomic percent). Common quaternary alloys, such as Ti-Al-Cr-Nb, Ti-Al-Mn-Nb, and Ti-Al-W-Si alloys, typically contain between 45% and 48% Al, and therefore can experience either primary beta phase or primary alpha phase solidification. The beta-stabilizing elements in these alloys, such as Cr, W and Mn, can promote differences in solidification mode versus binary alloys with the same Al content. Recent studies by Muraleedharan, et al. [11] and DeGraef et al. [12] on the solidification of cast Ti-48Al-2Cr-2Nb have suggested that for Al compositions within the specification range (> 47% Al) this alloy type generally solidifies as alpha phase, particularly at faster cooling rates that would be experienced during welding. As with conventional titanium alloys, gamma titanium alloy castings and welds solidify as columnar grains that grow parallel to the direction of heat flow and increase in size with a decrease in the solidification/cooling rate. On a microscopic scale, solidification occurs dendritically, with microsegregation promoting an enrichment of Ti and a depletion of Al in the dendrite cores, and an enrichment of Al and depletion of Ti in the last-to-solidify interdendritic regions. Although a cellular-dendritic or columnar-dendritic structure typically grows approximately parallel to the columnar grains, the unexpected presence of equiaxed dendrites in distinctly columnar grains has commonly been observed in both castings and welds [11].

Regardless of the solidification mode, solid-state phase transformations that occur during continuous cooling generally result in a fully-alpha microstructure at elevated temperatures that transforms to an alpha + gamma microstructure on cooling. Several investigators have examined the influence of continuous cooling rate on solid-state phase transformation behavior, particularly in binary Ti-Al alloys. Vasudevan and co-workers [13-16] and Kumagai et al. [17,18] have shown that at high cooling rates such as those experienced during quenching the alpha phase is retained down to room temperature and orders to form metastable alpha-two phase. At slower cooling rates (e.g., between 10-100 ^{o}C/s for Ti-48%Al), alpha decomposition occurs massively to a fine, acicular (needle-like) morphology that contains many stacking faults and a high dislocation density. A further decrease in cooling rate results in decomposition to a Widmanstatten-type morphology, and ultimately to a lamellar alpha-two/gamma constituent. It is not uncommon for microstructures to contain combinations of phases and gamma phase morphologies, such as retained alpha-two phase, massive gamma and Widmanstatten gamma phase. Commercial alloys, such as Ti-48Al-2Cr-2Nb and Ti-48Al-2Mn-2Nb, have shown similar phase transformation behavior to the binary alloys [17,18].

3. JOINING OF GAMMA TITANIUM ALUMINIDES

3.1 Gas Tungsten-Arc Welding (GTAW)

An early evaluation of the GTAW of gamma titanium aluminides at GE Aircraft Engines was stimulated by their strong interest in producing high quality, investment cast gamma titanium aluminides for structural applications. A study by Kelly [19] simulated the foundry weld repair of Ti-48Al-2Cr-2Nb gamma titanium aluminide castings using the manual GTA welding of short U-groove joints and HIP dimples in cast + HIP'ed

slabs ranging in thickness from 3 to 9 mm. Base metals exhibited Al contents somewhat below the nominal 48 at% (46.6 and 47.6 at%) and the filler metal exhibited a relatively high Al content of 50.5 at%. Welds were produced with and without a preheat of up to 600^{o}C and with two different welding current and voltage combinations that provided both low and high weld heat inputs. Note that the relatively short length of the welds and welding practice with no interpass time delay, and therefore negligible workpiece cooling, provided significant preheat to each pass that reduced thermally-induced stresses in the weld coupons, even for the low heat input welding conditions.

Results showed that crack-free single and multi-pass groove welds and dimple repairs could readily be produced without preheat for cast slabs that were heat treated prior to welding (1300^{o}C/20 hrs) to optimize base metal ductility. In contrast, welds produced in the HIP'ed or HIP'ed + 982^{o}C/1 hr heat-treated conditions, even with preheat to 316^{o}C, experienced cracking. Microstructure analysis showed an as-welded fusion zone microstructure to be comprised of lamellar alpha-two + gamma constituent, with evidence of Cr-enriched B2 phase. Postweld heat treatment at 1300^{o}C/20hrs promoted appreciable recrystallization to a predominantly equiaxed gamma phase microstructure, with only small amounts of alpha-two phase, which is consistent with the high Al content of the filler metal. B2 phase present in the as-welded microstructure was no longer evident following heat treatment.

This early work demonstrated that crack-free GTA welds can be produced in Ti-48Al-2Cr-2Nb titanium aluminide castings without external preheat, but only after the casting had been heat treated to optimize its ductility. Kelly suggests that the relatively high energy input associated with manual GTA welds, the welding of relatively small

workpieces, and a welding procedure that was continuous, resulted in lower weld zone cooling rates and reduced thermally-induced stresses versus automatic GTAW or the manual GTAW of large structural components that would promote more rapid weld cooling rates, higher weld stresses, and solid-state cracking.

Mallory et al. [20,21] investigated microstructure evolution in the HAZ of a single-pass GTA weld produced manually in a Ti-48.7Al-2.0Cr-1.9Nb forging using a nominally matching filler metal chemistry. In order to prevent cracking welding was performed using a preheat of 800^{o}C. Light, SEM and TEM microscopy revealed on-heating transformation of the predominantly equiaxed gamma + grain boundary alpha-two base metal microstructure across the weld HAZ (Fig. 3). In the far-HAZ (Fig. 3a), acicular alpha-two platelets were observed to emanate from gamma grain boundaries, often forming a lamellar-like constituent within a single gamma grain. The lamellar alpha + gamma microstructure produced on heating in the far HAZ has been described by Kim [22] as a Type III lamellar structure, in which adjacent gamma regions exhibit the same crystallographic orientation. Additional singular alpha-two platelets were observed to auto-partition the gamma grains, resulting in increasingly smaller alpha-two platelets. Higher peak temperatures experienced nearer to the weld fusion line promoted increased alpha platelet formation (Fig. 3b) and ultimately in the near-HAZ coalescence into single alpha grains (Fig. 3c). Upon weld cooling, these alpha regions transformed to a fine, lamellar alpha-two + gamma constituent. This transformation product has been described by Kim as a Type I lamellar microstructure, in which adjacent gamma plates are not of the same crystallographic orientation, but rather are twin related.

Examination of the weld fusion zone using SEM/EDS analysis showed a dendritic solidification structure and compositional coring produced during non-equilibrium solidification through cascading peritectics on the Ti-Al phase diagram (Fig. 4). EDS analysis indicated enrichment of Ti and depletion of Al in the dendrite cores relative to the dendrite intersticies. Light and transmission-electron microscopy of the fusion zone revealed a predominantly lamellar gamma + alpha-two microstructure similar to that observed in the near-HAZ, with occasional equiaxed gamma grains and Widmanstatten structure. The aforementioned microsegregation did not appear to markedly impact this transformed lamellar microstructure. Mallory et al. did not perform tensile testing on the GTA weldment, however, they did observe a significant increase in hardness from diamond pyramid hardness (DPH) 225 in the unaffected base metal to DPH 325 in the near-HAZ, and DPH 350 in the fusion zone, suggesting a high joint efficiency, but the potential for reduced weld zone ductility and fracture toughness.

Mallory et al. [20] also utilized a Gleeble 1500 thermo-mechanical system to generate simulated GTA weld HAZ microstructures in Ti-48Al-2Cr-2Nb for conditions that paralleled those calculated for the actual GTA weld described above. For a range of peak HAZ temperatures between the eutectoid and alpha-transus temperatures, they observed microstructural characteristics and hardnesses that generally compared well to those observed in the actual weld. They further observed evidence of sluggish gamma phase dissolution kinetics on heating, which suggests that the isotherm bounding the far-HAZ and near-HAZ regions in the welds exceeds the equilibrium alpha-transus temperature.

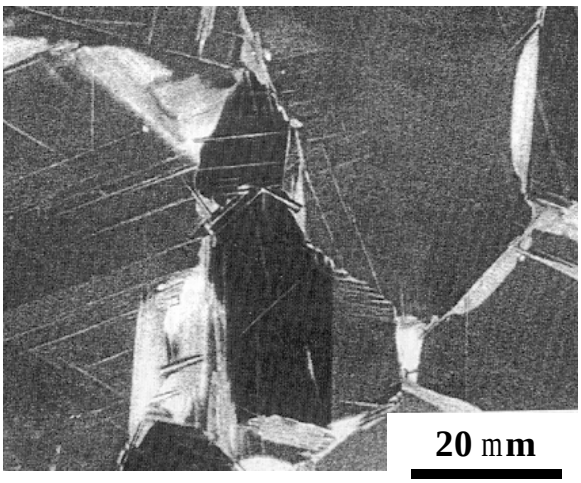

(a)

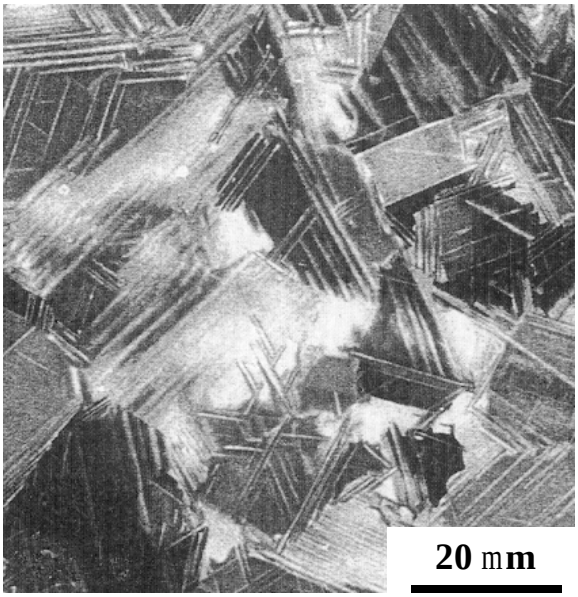

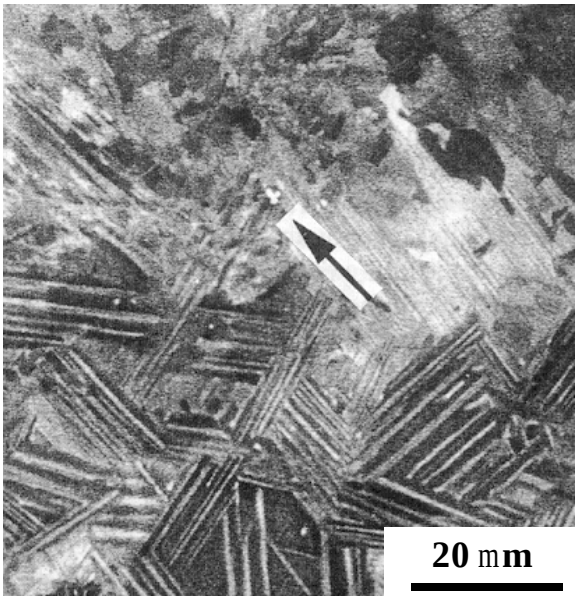

(b) (c)

Figure 3. SEM/BSE micrographs across the heat-affected zone of a single-pass GTA weld in forged and heat-treated Ti-48Al-2Cr-2Nb [21]: (a) far-HAZ nearer to unaffected base metal; (b) far-HAZ nearer to fusion line; (c) boundary between far and near-HAZ.

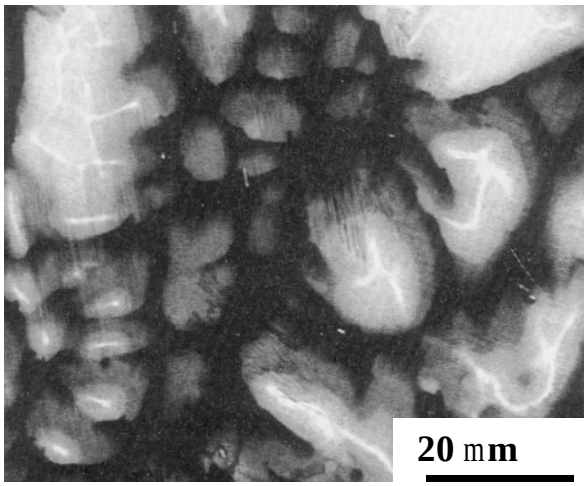

Figure 4. SEM/BSE micrograph of the weld fusion zone in a single-pass GTA weld in forged and heat-treated Ti-48Al-2Cr-2Nb [21].

Work performed at TWI by Threadgill and Dance [23] examined the GTA welding of a 5 mm thick cast Ti-48Al-2Mn-2Nb alloy, and observed significant problems with solid-state cracking particularly at the weld start and stop locations. They attributed these cracks, which initiated near the fusion line and propagated perpendicular to the welding direction into the base metal, to thermal stresses that are highest at these locations, and to stress concentrations in the weld crater. Based on preliminary results, they suggest that preheating of the workpiece above 500^{o}C would be required to eliminate cracking. As with previous investigations of the autogenous GTA welding of Ti-48Al-2Cr-2Nb [20,21], they observed significant difficulty in achieving weld penetration. Increasing the welding current, even when using helium as the shielding gas, promoted a wider fusion zone with a negligible increase in penetration depth. Although not confirmed, they attribute this effect to the nature of fluid flow in the weld fusion zone, and suggest that penetration may be enhanced through the addition of surfactants that modify the temperature dependence of the surface tension on the weld pool surface, and correspondingly the fluid flow in the weld pool. Microstructure analysis revealed a fine lamellar alpha-two + gamma fusion zone microstructure, similar to that observed by Mallory [20,21], over a range of preheat temperatures from 100 to 500^{o}C. In the weld HAZ they observed non-parallel alpha-two laths. Although they did not report on weld mechanical properties, they did note a decrease in the weld zone hardness with an increase in preheat due to lower cooling rates.

Hurta et al. [24] applied GTA welding to produce porosity-free weld joints between exhaust valve stems and disks of a Ti-46Al-1.5Cr-0.9Nb-0.1Si alloy. They

noted a strong tendency for solid-state cracking and recommended preheating of the blanks prior to welding. Metallurgical analysis of the welds was not presented.

Acoff and coworkers studied the microstructure and hardness of autogenous GTA spot welds produced in extruded Ti-46Al-2Cr-2Nb-0.9Mo [25,26] and cast + HIP'ed Ti-47.9Al-2.0Cr-2.0Nb [26]. Welds were produced on thin sheet coupons using a range of welding currents from 45-75 amperes and identical arc times of 3 seconds in order to investigate the influence of weld heat input and cooling rate on microstructure evolution. Subsequent to welding, coupons were given a low temperature (615^{o}C/2hrs) stress-relief heat treatment. Solid-state cracking was observed in the weld fusion zones. As in previous studies, the total fusion zone crack length decreased with an increase in weld heat input, with crack-free welds produced at the highest heat input.

Fusion zone solidification structures were examined using SEM/BSE analysis, and exhibited columnar grain and directional dendritic solidification structures for the low and intermediate current levels. At higher current levels, a coarser dendritic structure appeared directional near the fusion line, but less directional and more equiaxed near the fusion zone centerline.

Both the cast Ti-48Al-2Nb-2Cr alloy and the wrought Ti-46Al-2Cr-2Nb-0.9Mo alloy exhibited a predominantly equiaxed gamma base metal microstructure, with the gamma grain size of the extruded product being appreciably finer. The weld HAZ experienced a transformation similar to that reported by Mallory et al. [20,21], with acicular alpha-two platelets forming in the far-HAZ, and a fully-transformed near-HAZ comprised of fine, lamellar alpha-two + gamma constituent. The fusion zone was likewise comprised principally of fine, lamellar constituent, with occasional evidence of

interdendritic gamma promoted by the non-equilibrium peritectic solidification. Energy-dispersive X-ray analysis of the fusion zones indicated Cr enrichment at dendrite cores and Cr depletion within the interdendritic regions for low energy inputs, and a reversal of this segregation for higher heat input welds that exhibited a more equiaxed dendrite morphology. The origin of this segregation reversal is unclear. Microhardness testing showed an increase in hardness from the base metal, across the HAZ, and into the fusion zone, with the average fusion zone hardnesses appreciably greater than those of the base metals. Although the base metal hardness of the wrought alloy was appreciably greater than the cast alloy, (average of DPH 280 versus DPH 227) the weld fusion zone hardnesses were quite comparable (average of DPH 482 versus DPH 473). For both alloys the fusion zone and HAZ hardnesses did not vary significantly with the weld heat input.

In a subsequent investigation, Acoff and Arenas [27] examined the microstructure and hardness of continuous GTA welds produced in 2 mm thick sheet machined from a HIP'ed + heat-treated Ti-48Al-2Cr-2Nb investment casting using different current levels ranging from 75-95 A and a continuous 3 mm/s travel rate. Fusion zone solidification structures exhibited predominantly columnar-dendritic growth from the fusion line up toward the weld top surface, with the dendrite coarseness and the quantity of interdendritic gamma phase increasing with increasing heat input. Consistent with previous studies, the dendrite cores exhibited an enrichment of Ti and a depletion of Al relative to the dendrite intersticies. In contrast to previous studies of GTA spot welds, EDS analysis showed no segregation of Cr between the dendrite cores and intersticies. The weld HAZ was very narrow and difficult to distinguish because of the steep

temperature gradient across this region. Although transformed microstructures in the fusion zone and HAZ were not examined in this investigation, it is anticipated that they would be comprised of very fine lamellar alpha-two + gamma constituent, or possibly a fine Widmanstatten gamma at lower heat inputs. Hardness traverses across the weld zones showed a rapid change in hardness at the fusion line due to the appreciably finer transformed microstructure in this region versus the coarser, predominantly lamellar base metal microstructure. Interestingly, the fusion zone hardness increased appreciably with an increase in heat input, which is in contrast to previous spot-welding tests that showed no change. Without detailed analytical-electron microscopy of the fusion zone microstructure it is not possible to determine the origin of this hardness change.

Most recently, Acoff and co-workers [28] evaluated the postweld heat treatment response of autogenous GTA welds produced in 3 mm thick Ti-46.8Al-1.8Nb-1.8Cr sheet that was sectioned from a HIP'ed and heat-treated investment casting. Following postweld stress relief heat treatment at 900^{o}C/2 hr, welds were postweld heat treated at 1000^{o}C and 1200^{o}C for 1, 10 and 48 hrs. Postweld heat treatment at 1000^{o}C for one hour promoted transformation of the fusion zone to a duplex structure comprised of recrystallized, equiaxed gamma grains, and lamellar alpha-two + gamma constituent. Increasing the heat treatment time to 10 hrs promoted increased recrystallization and a microstructure comprised principally of equiaxed gamma grains. Postweld heat treatment at 48 hours significantly reduced the proportion of equiaxed gamma grains through the nucleation of new lamellar regions at grain boundaries, perhaps driven by discontinuous coarsening. Heat treatment at 1000^{o}C had a negligible effect on the base metal microstructure. PWHT at 1200^{o}C/1 hr promoted appreciable recrystallization and

transformation to equiaxed gamma grains, which increased significantly for PWHT for 10 hrs. Heat treatment at 1200°C/48 hrs promoted an increase in the gamma grain size, and the formation of Widmanstatten alpha-two plates within the gamma grains.

As observed in previous studies, hardness increased significantly across the weld zone from the base metal to the fusion zone. Transformation from what was probably a fine, lamellar fusion zone microstructure in the as-stress-relieved microstructure, to an increasingly equiaxed gamma microstructure following postweld heat treatment at both temperatures for 1 and 10 hrs promoted appreciable softening. Microstructural changes that occurred during postweld heat treatment for 48 hrs, including the precipitation of alpha-two phase within the recrystallized gamma grains during the heat treatment at 1200°C, promoted an increase in fusion zone hardness versus the 10 hr heat treatment. Generally, the fusion zone hardness levels were reduced slightly more for the 1200°C versus the 1000°C heat treatment for identical heat treatment times. Postweld heat treatment did not significantly change the base metal hardness, which was consistent with microstructural observations.

Xu et al. [29] investigated the influence of weld preheat temperature on the solid-state cracking susceptibility and microstructure in GTA bead-on-plate and butt welds produced on 2 mm thick Ti-45Al-2Nb-2Mn-0.8TiB_2 sheet. They observed a nearly linear decrease in cracking with an increase in preheat temperature, with cracking totally eliminated for temperatures of 250°C and above. As with many previous investigators, they also observed a delayed cracking behavior, suggesting the occurrence of a combined environmental/residual stress cracking mechanism, and recommended postweld stress relief heat treatment immediately following welding. Electron microscopy analysis of the

GTA weld fusion zone microstructures showed that the most rapidly cooled welds produced with no preheat contained a predominantly retained alpha-two and massively-transformed gamma phase microstructure. Intermediate cooling rates associated with preheat temperatures of 100°C to 200°C promoted transformation to microstructures comprised of massive gamma phase and a finely-spaced lamellar alpha-two + gamma constituent, while the slowest cooling rates for preheats of 250°C and greater promoted decomposition to a nearly entirely lameller microstructure. Xu et al. propose that the retained alpha-two and massively-transformed gamma phase microstructures are inherently more brittle than the finely-spaced lamellar alpha-two + gamma microstructures, and that this brittleness, combined with the higher residual stresses developed at higher weld cooling rates, promote greater cracking susceptibility.

Jensen et al. [30] investigated the multi-pass GTAW of 12.7 mm thick Ti-48Al-2Nb-2Cr cast + HIP'ed plate. The microstructure and hardness of the weld, which was produced using a preheat and minimum interpass temperature of 200°C, were investigated following a postweld stress-relief heat treatment at 980°C/2 hrs, and subsequent postweld heat treatments at 1050°C, 1150°C and 1250°C for 5 hrs. Light microscopy examination of the weld revealed the individual weld passes (Fig. 5), and the presence of white, featureless regions at weld pass boundaries. Examination of the weld zone using SEM/BSE clearly revealed the dendritic solidification structure of the weld, and an absence of this structure in the white band regions (Fig. 6). Energy-dispersive X-ray analysis and electron-microprobe analysis of the banded regions showed a depletion of aluminum down to 45 at% in the banded regions, versus approximately 47 at% in the bulk fusion zone. TEM analysis of the weld fusion zone revealed a combination of

recrystallized gamma grains and fine lameller colonies in the bulk fusion zone, and very fine lamellar alpha-two + gamma constituent in the banded region (Fig. 7). Postweld heat treatment promoted further recrystallization of the bulk fusion zone regions, but did not recrystallize the lamellar banded regions, which is consistent with their lower Al content and greater microstructural stability. Diamond pyramid hardness of the banded regions was appreciably higher than that of the bulk fusion zone (DPH 382 vs. DPH 311), which was consistent with its fine lamellar microstructure. Although PWHT softened both weld regions, the fusion zone hardness remained well above that of the base metal. Fracture toughness testing of the fusion zone determined the as-welded microstructure to be less tough than the base metal (9.8 MPa-$m^{1/2}$ versus 18 MPa-$m^{1/2}$), and heat treatment at 1050^{o}C/5hr and 1250^{o}C/5hr reduced the fusion zone toughness to 3.8 and 4.2 MPa-$m^{1/2}$, respectively, which is consistent with the transition from a primarily lamellar microstructure to a predominantly equiaxed gamma microstructure.

A subsequent study by Breeding and co-workers [31] that utilized higher Al filler metals (46.7 and 47.6 at% Al) was successful in producing multi-pass GTA welds in 12.5 mm thick Ti-48Al-2Nb-2Cr plate that did not exhibit compositional banding observed in the previous welds. As shown in Fig. 8, postweld heat treatment of these welds resulted in a microstructure comprised of lamellar constituent and equiaxed gamma grains, with gamma grains located primarily at the boundaries between weld passes and along colony and grain boundaries.

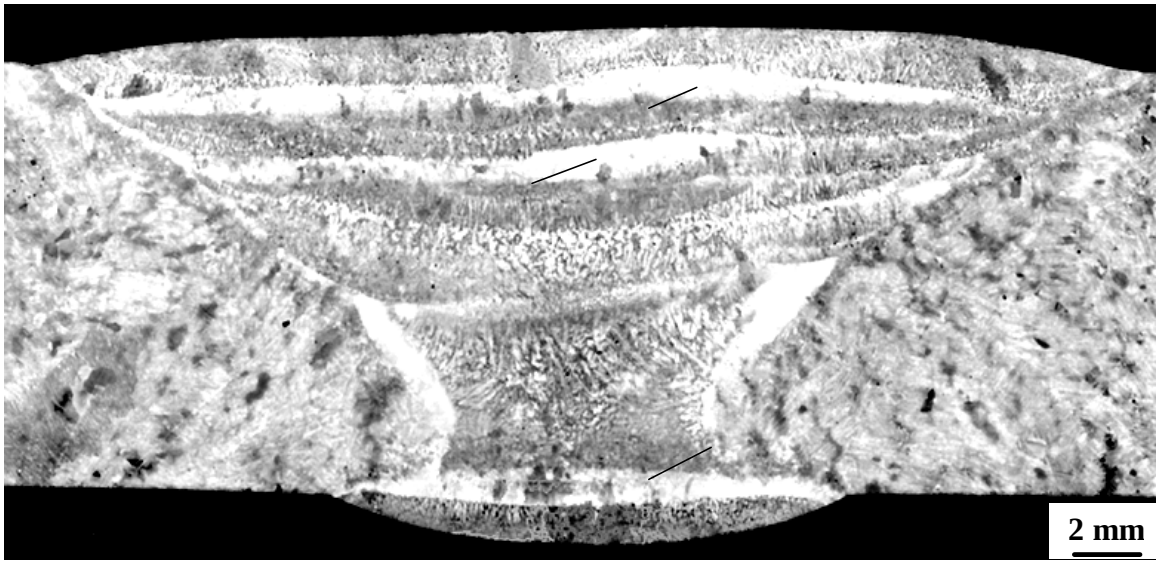

Figure 5. Light micrograph of multipass GTA weld in investment cast + HIP'ed + heat- treated Ti-48Al-2Cr-2Nb. Arrows indicate macroscopic bands located at boundaries between weld passes [30].

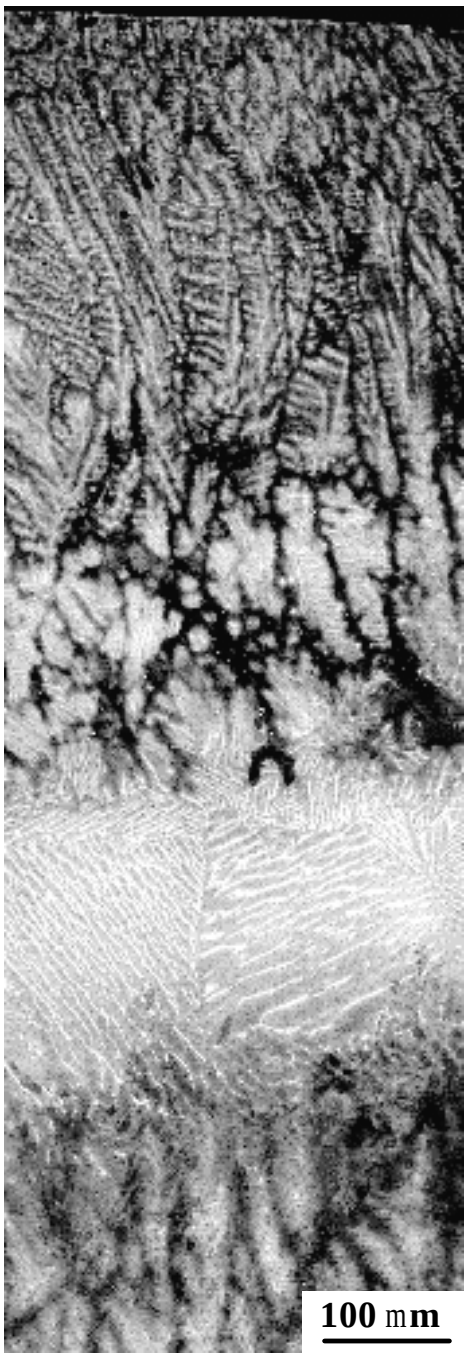

Figure 6. SEM/BSE micrograph showing fusion zone solidification structure of multipass GTA weld in investment cast + HIP'ed + heat-treated Ti-48Al-2Cr-2Nb [30].

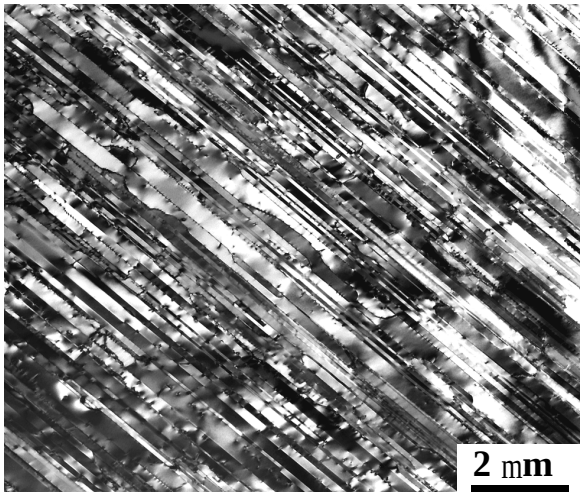

(a)

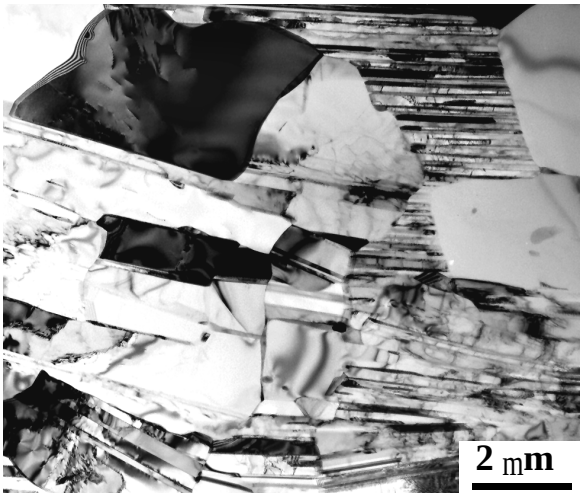

(b)

Figure 7. TEM bright-field micrographs of GTA weld fusion zone in investment cast + HIP'ed + heat–treated Ti-48Al-2Cr-2Nb: (a) banded region; (b) bulk fusion zone.

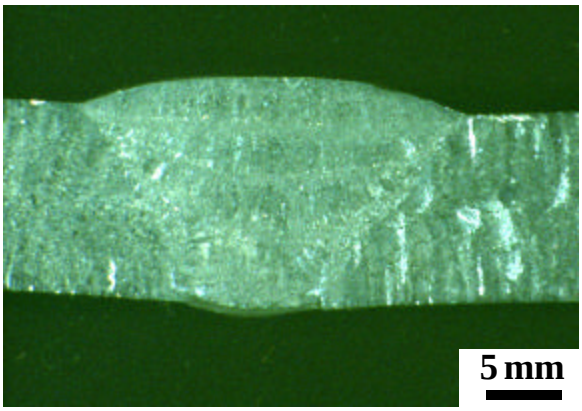

(a)

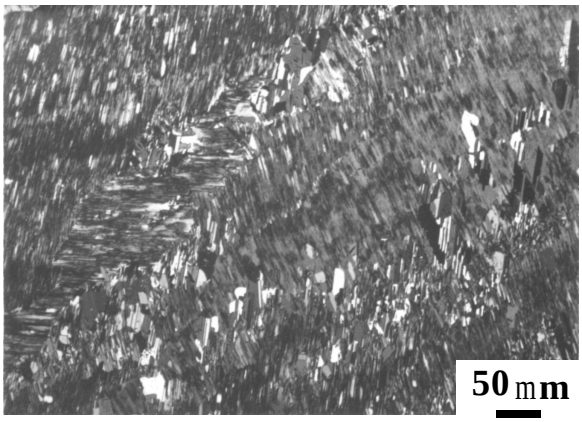

(b)

Figure 8. Light micrographs of multipass GTA weld in investment cast + HIP'ed + heat-treated Ti-46.7Al-2Cr-2Nb using Ti-48/2Al-2Cr-2Nb filler metal and postweld heat-treated at 1093^{o}C/5hrs [31].

As indicated previously, the autogenous GTA welding of gamma titanium aluminides is characterized by poor penetration that cannot be overcome through welding parameter control. Recent work by Breeding et al. [32] has shown that halide-based fluxes currently under development by EWI significantly enhance fusion zone penetration. As shown in Fig. 9, application of the flux allowed nearly full penetration through a 10 mm thick plate, a penetration increase of nearly three times versus a weld produced with identical welding conditions but without the flux. This increase is attributed primarily to a change in the fluid flow direction at the top surface of the weld, from the center under the arc outward, that would promote a wider, shallower pool, to from the outer edge of the weld inward toward the center and downward under the arc, that would promote a narrower, deeper penetrating weld pool. In addition to significantly enhanced penetration, the flux-produced weld further exhibited a greater resistance to solid-state cracking. Detailed microstructure analysis using TEM indicated no residual effects of the flux on the weld chemistry or microstructure.

3.2 Electron Beam Welding (EBW) and Laser Beam Welding (LBW)

Electron beam welding offers several advantages over arc welding processes in the joining of aerospace structures, including deep-penetration capabilities with minimal requirements for joint preparation and without the requirement for a filler metal, comparatively low residual stress and distortion, and a high degree of weld cleanliness since welding is performed in a high vacuum. A potential disadvantage of EBW is the very rapid cooling rates typically experienced, up to several thousand ^{o}C/s, which can promote the formation of nonequilibrium, metastable microstructures that are highly susceptible to solid-state cracking during weld cooling, exhibit reduced mechanical

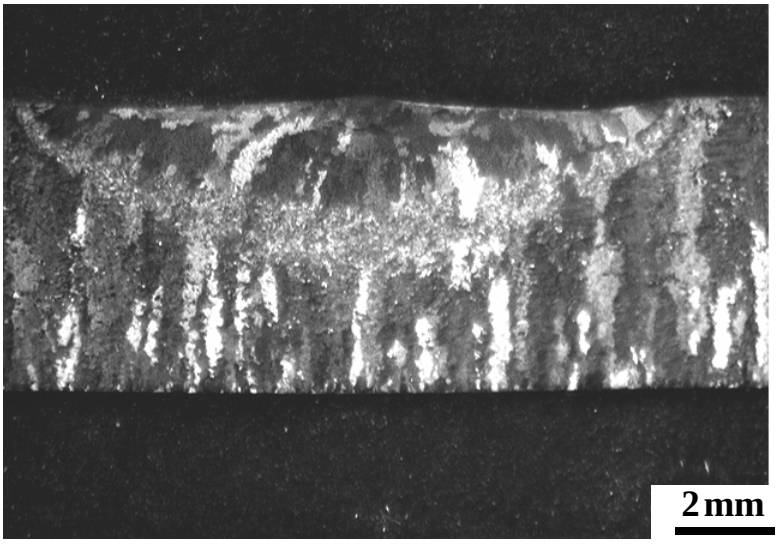

(a)

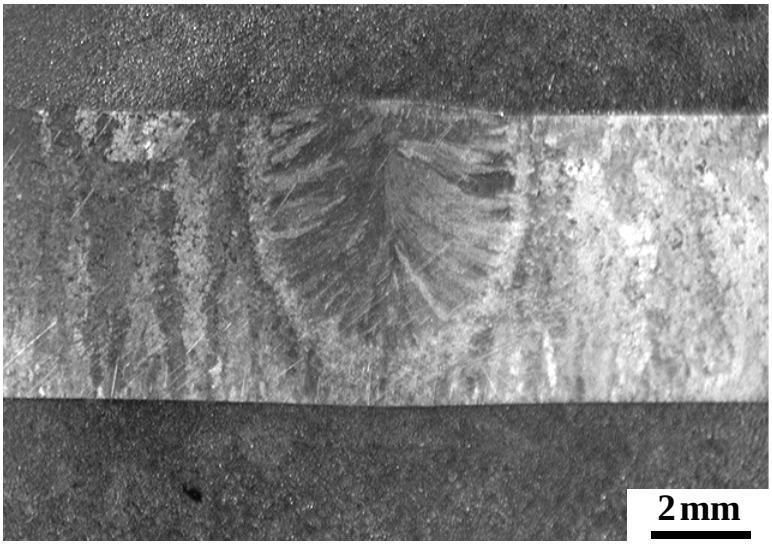

(b)

Figure 9. Light macrographs of autogenous GTA welds in 10 mm thick Ti-46.7Al-2Cr-2Nb: (a) without flux; (b) with halide-based active flux [32].

properties relative to the microstructurally-optimized base metal, or that exhibit thermal instability that can be problematic in subsequent elevated-temperature applications.

Early EBW studies by Patterson et al. [33,34] investigated the weldability of Ti-48 at%

Al-6.5 vol% TiB_2. This alloy, which was produced using the XD process, contains TiB_2 particulate that promotes grain refinement during casting and thermo-mechanical processing. Full-penetration, autogenous welds were produced on 2.5 mm thick machined stock with the weld thermal cycle controlled by varying the beam power, traversing rate, and preheat temperature. They found that well contoured, high-quality welds could be generated using EBW, and determined a strong correlation between the weld cooling rate between 1400°C and 800°C, and the frequency of solid-state cracking (Fig. 10). Although solid-state, transgranular cracks were observed to initiate at the boundary between the fusion zone and the HAZ and propagate transverse to the welding direction, and be nearly equidistant apart along the weld length, this problem could be eliminated if calculated HAZ cooling rates (at the fusion boundary) were maintained below about 300°C/s. Light microscopy analysis of weld fusion zones found a decrease in the volume fraction of lamellar alpha-two + gamma constituent and an increase in the volume fraction of acicular Ti-B phase with an increase in cooling rate, and TEM analysis revealed that the lamellar structure was replaced with equiaxed gamma grains. X-ray diffraction studies found a significant increase in the volume percentage of alpha-two phase with an increase in weld cooling rate, from 33% in the slow-cooled weld (150°C/s) to 78% in the fast-cooled weld (1675°C/s). Patterson attributed the solid-state transgranular cracking to thermally-induced stresses that exceeded the material's yield strength in a temperature range of limited ductility, with an increase in cooling rate promoting an increase in stress. A second mechanism that promoted cracking at higher cooling rates was associated with the formation of a less ductile, and more crack-susceptible microstructure at higher cooling rates. Indeed, this mechanism was supported

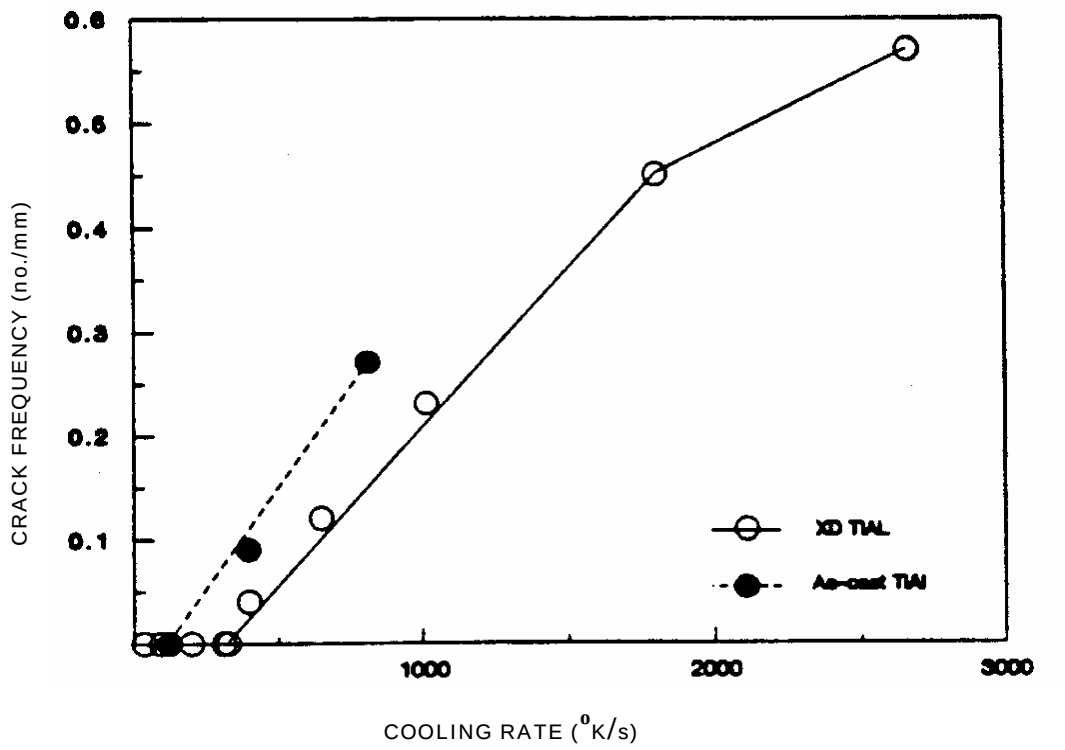

Figure 10. Solid-state cracking frequency (number of cracks per mm length of weld) versus calculated average weld HAZ cooling rate from 1400°C to 800°C) for EB welds produced in Ti-48Al-6.5vol% TiB_2 and cast Ti-48 at% Al [34].

by their observation of a high proportion of retained alpha-two phase in welds produced with low preheat and a high cooling rate, since alpha-two phase volume fractions of greater than 20% have been shown by Kim (35) to embrittle TiAl .

The results of a parallel EBW study by Patterson et al. [34] on a cast Ti-48 at% Al alloy compared well with those of the XD-type alloy. As with the XD-type alloy, they determined a critical cooling rate of approximately 100^{o}C/s below which solid-state cracking did not occur. Cracking susceptibility was again attributed to the combined effects of a high cooling rate promoting both an increase in thermal stresses across the weld, that ultimately exceed the fracture stress, and a weld zone microstructure of limited ductility. They attributed the lower critical cooling rate of the cast Ti-48 at% Al alloy versus the XD-type alloy to its coarser grain size and an absence of TiB_2 particles, which would slow the alpha-to-gamma phase transformation and promote an increased volume percentage of retained alpha-two phase at room temperature.

Godfrey et al [36] examined EB welds produced in 5 mm thick cast T-48Al-2Mn-2Nb with preheat temperatures of 150-900^{o}C provided by in-situ rastering of the electron beam over the region to be welded. Welding parameters remained constant for all welds. They determined that preheats of greater than 500^{o}C were required to prevent solid-state cracking. Appreciable microstructure analysis was performed using light and transmission-electron microscopy to investigate phase transformations and corresponding microstructure evolution during weld cooling. At low preheats, and the highest weld cooling rates, they observed retained alpha-two phase with fine gamma laths. The retained alpha-two regions, which were observed for preheat temperatures of below 500^{o}C, were located primarily at the fusion zone/HAZ boundary, which was attributed to

solidification-induced segregation effects in the fusion zone. As the preheat temperature increased, and the cooling rate decreased, a transition in transformation products occurred to combinations of massively-transformed gamma (no preheat to 700^{o}C), Widmanstatten gamma (250^{o}C to 700^{o}C), and finally lamellar alpha-two + gamma constituent (500^{o}C to 900^{o}C), which was predominant for a 900^{o}C preheat temperature. These microstructural results correspond well with previous continuous-cooling phase transformation studies in gamma titanium aluminides. Interestingly, the authors attribute the increase in cracking susceptibility with an increase in weld cooling rate exclusively to an increase in the thermal stresses, and do not suggest a microstructural influence.

Chaturvedi and co-workers [37] investigated the EBW of a Ti-45Al-2Nb-2Mn-0.8 vol.% TiB_2 alloy, focusing on the development of relationships between the weld cooling rate, fusion zone and HAZ phase transformations and microstructure evolution, and susceptibility to solid-state cracking. Partial-penetration EB welds were produced on small coupons 12 mm in thickness, with the weld cooling rate controlled by varying the welding parameters and preheat provided by a defocused electron beam. As expected, welds produced at high cooling rates, exceeding 1000^{o}C/s (calculated average rate between 1300^{o}C and 1000^{o}C) exhibited extensive solid-state cracking, propagating from the fusion zone into the base metal at the highest cooling rates. TEM analysis of weld fusion zones produced at a cooling rate of 1120^{o}C/s revealed a fully-retained alpha-two phase microstructure, while a slower rate of 580^{o}C/s resulted in partial transformation to massive gamma phase. Gleeble thermal simulation studies performed concurrent with the EB welding trials generated simulated near-HAZ microstructures over a range of cooling rates, and corroborated the EB weld characterization studies by more clearly

establishing the relationship between cooling rate and transformation behavior, in particular, retention of the alpha-two phase. These studies also revealed the initiation of cracks in the alpha-two phase in two-phase alpha-two + gamma microstructures. This work suggested that a reduction in the EB weld cooling rate to 250^{o}C/s would promote complete decomposition of the alpha phase to massive gamma and lamellar alpha-two + gamma constituent, which would be expected to be crack resistant. The subsequent optimization of welding parameters to provide this cooling rate did, indeed, result in the production of crack-free welds that exhibited a fusion zone microstructure comprised primarily of lamellar constituent, with a small volume percentage of massive gamma phase. Consistent with the observations of Patterson et al. [33,34], they concluded that the selection of welding parameters and cooling rates that promote complete decomposition of the high-temperature alpha phase will prevent weld cracking by providing a transformed microstructure that is capable of accommodating strains generated by thermally-induced weld stresses. It should be noted that their work did not indicate an effect of needle-like phases associated with the TiB_2 particles on phase transformations or susceptibility to solid-state cracking.

A subsequent study by Chaturvedi and co-workers [38] extended the previous EB welding and Gleeble thermal simulation studies to evaluate the role of on-cooling weld phase transformations on the weldability of cast and heat-treated Ti-45Al-2Nb-2Mn and Ti-48Al-2Nb-2Mn alloys. As shown in Figure 11, the solid-state cracking susceptibility of the Ti-45Al-2Nb-2Mn alloy increased linearly with cooling rate to approximately 660^{o}C/s, sharply increased at that rate, and increased linearly at higher cooling rates. They suggest that the continuous linear increase in cracking with cooling rate results in

part from an increase in thermal stresses with increased cooling rate, but that the discontinuity in cracking susceptibility originates from a significant microstructural change that occurs at that cooling rate. TEM examination of welds produced at cooling rates of 730°C/s and above revealed a fully-retained alpha two-phase microstructure, which is known to be extremely brittle and crack sensitive. At a cooling rate of 590°C/s, which showed appreciably less cracking, partial decomposition occurred to massive gamma phase. As in their previous study, they utilized Gleeble simulation studies to determine a cooling rate for which full decomposition of the alpha phase occurred, which for this alloy was found to be 240°C/s. EB welds subsequently produced using this slower cooling rate did indeed exhibit the predicted, fully-transformed microstructure and an absence of cracking. A subsequent Gleeble study on Ti-48Al-2Nb-2Mn revealed faster on-cooling alpha decomposition kinetics, and correspondingly that a higher cooling rate of 400°C/s was required to suppress decomposition of the alpha phase. Subsequent EBW studies confirmed that the use of a cooling rate of 380°C/s produced a crack-free weld microstructure comprised of massive gamma phase and lamellar alpha-two + gamma constituent. Based on these analysis they conclude that although cracking is influenced by welding stresses, that microstructure, and particularly the presence of retained alpha-two phase, plays the dominant role in determining solid-state cracking susceptibility. In this context, they suggest that CCT diagrams would be very useful tools for predicting crack-free welds.

EBW studies described above were typically performed on small weld coupons due to material availability limitations, or the use of preheating/cooling rate control techniques that restricted the size of the workpiece. In contrast, work by Kelly [39]

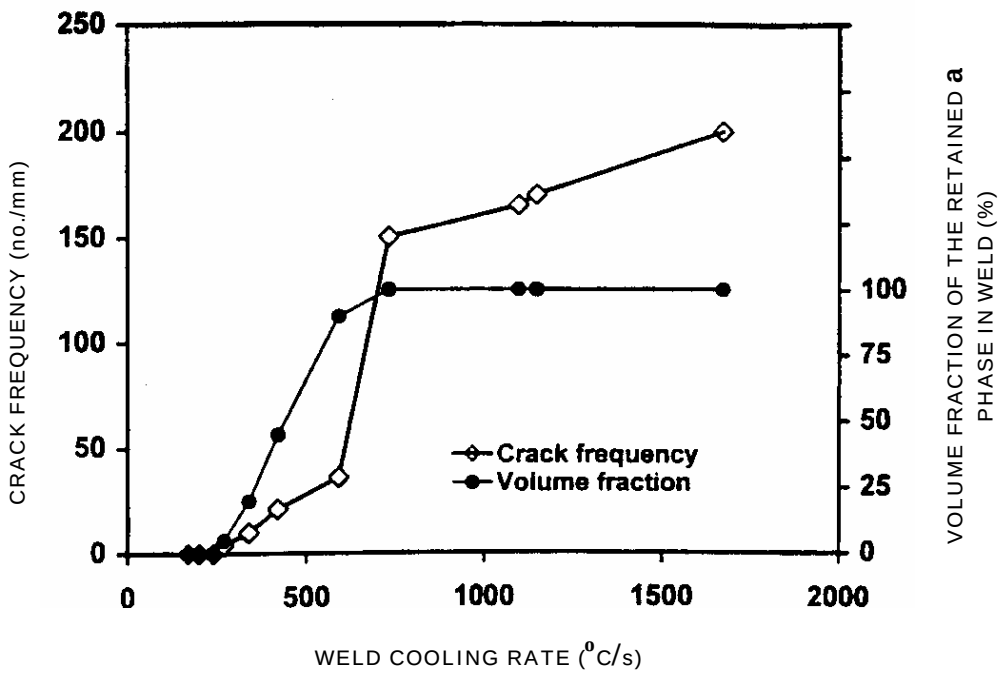

Figure 11. Solid-state cracking frequency (number of cracks/meter length of weld) and volume fraction of retained alpha-two phase in the weld versus calculated weld HAZ cooling rate (from 1350°C to 1000°C) for EB welds produced in Ti-45Al-2Nb-2Mn [38].

developed EBW techniques required to fabricate large-scale cast gamma titanium-aluminide components planned for utilization in NASA's proposed High Speed Civil Transport. Initial studies involved the production of butt welds between investment cast + HIP'ed + heat-treated Ti-48Al-2Cr-2Nb plates that were 250 mm x 100 mm x 12.5 mm in thickness. Full-penetration butt welds were produced in alloys containing between 46.3 and 48.3 at% Al using a specially constructed EBW system that contained a furnace within the vacuum chamber to provide weld preheat and postweld stress relief heat treatment. Kelly found that welds produced in a 47.1 at% Al alloy with a 650°C preheat did not crack immediately following welding, but did crack subsequent to their removal from the vacuum chamber. Postweld stress relief heat treatment at 871°C/2hr within the chamber prevented this apparent delayed cracking phenomenon. Based on a series of welding trials in which the postweld stress-relief temperature was varied, they determined that an 982°C/2 hr postweld stress relief heat treatment would consistently result in the production of defect-free welds for Ti-48Al-2Nb-2Cr alloys within the current alloy specification range for aluminum.

Using these welding procedures, a deep-penetration EB weld 75 mm in depth and 250 mm inches in length was produced between the major surfaces of two plates exhibiting a 5 mm inch wall thickness. Ultimately, a 150 mm deep penetration butt weld 400 mm in length was produced between the major surfaces of two 12.5 mm thick plates using a two-sided welding technique. (Fig. 12).

Jensen and co-workers [40] investigated the microstructure, properties and fracture behavior of several EB butt welds produced by Kelly [39] in 12.5 mm thick, HIP'ed and heat-treated Ti-48Al-2Cr-2Nb investment castings (Fig. 13). More

specifically, this work examined the influence of Al content between 46.3 to 48.3 at% and postweld heat treatment at 1050°C, 1150°C to 1250°C/5hrs on the microstructure, tensile and fracture toughness properties, and deformation and fracture characteristics of EB welds produced using the optimized techniques developed by Kelly (i.e, a weld preheat of 650°C and an immediate stress-relief heat treatment of 980°C/2hrs).

Heat inputs utilized during welding provided a calculated weld cooling rate of approximately 250°C/s between 1300°C and 1000°C, promoting transformation to a predominantly fine lamellar alpha-two + gamma microstructure in the as-welded fusion zone. Postweld stress-relief at 980°C/2hrs promoted recrystallization of the as-welded microstructures to equiaxed gamma grains, with the degree of recrystallization increasing with an increase in Al content (Fig. 14). As also shown in Fig. 14, the fusion zone microstructure was appreciably finer than the cast base metal microstructure. Postweld heat treatment at 1050°C/5 hr promoted further recrystallization and gamma grain growth (Fig. 15). Alpha-two phase in these microstructures was located principally at gamma grain boundaries and within gamma grains at previous dendrite intersticies. Increasing the postweld heat treatment temperature to 1150°C and 1250°C promoted transformation to acicular alpha-two plates within the gamma grains, particularly for the lower Al alloys (Fig. 16). Heat treatment of the low Al weld at 1250°C also promoted the formation of B2 phase. Postweld heat treatment at 1050°C promoted appreciable softening of the weld fusion zone due to recrystallization of the fine lamellar structure that remained in the stress-relieved condition, particularly for the lower Al welds that exhibited a higher volume fraction of lamellar constituent. At higher postweld heat treatment temperatures, precipitation of alpha-two phase promoted slight hardening, particularly in the lower Al

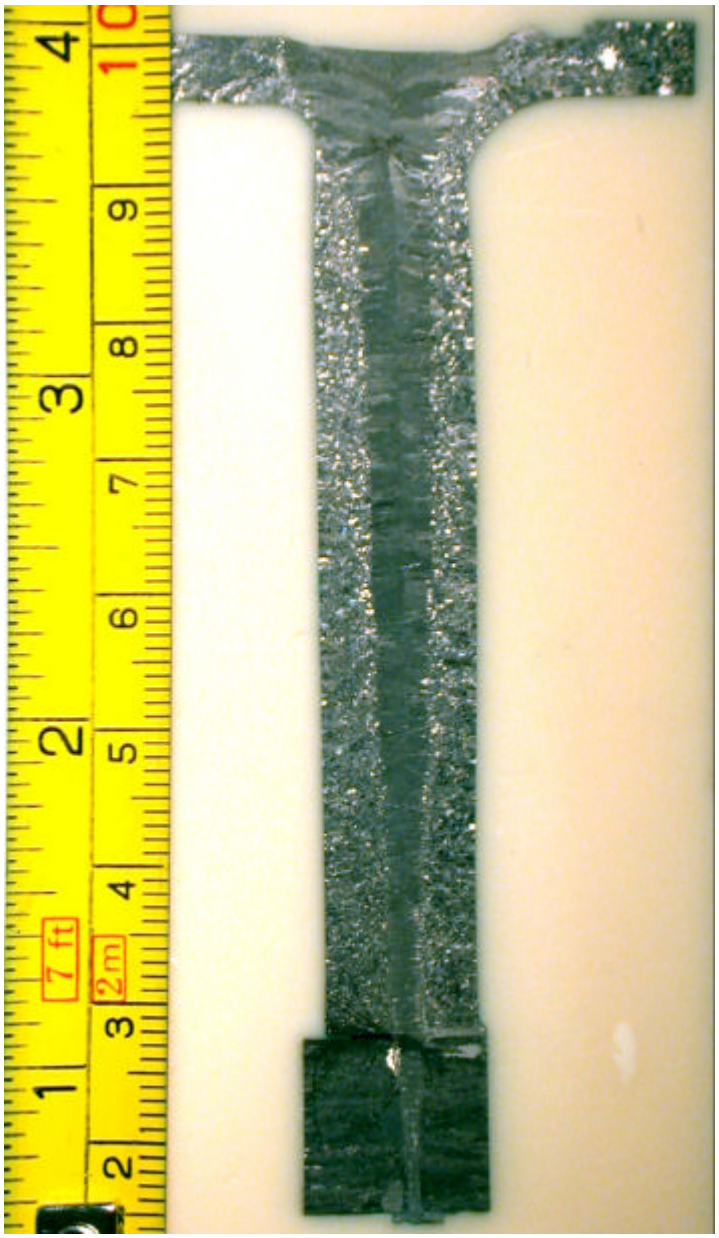

Figure 12. Deep-penetration, double-sided EB weld produced between 12.5 mm thick plates of Ti-48Al-2Cr-2Nb [39].

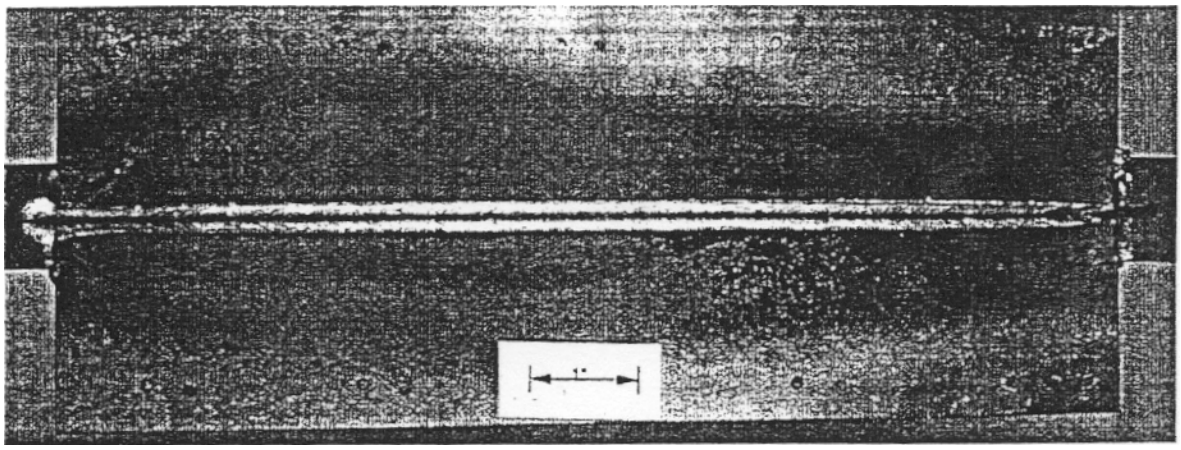

(a)

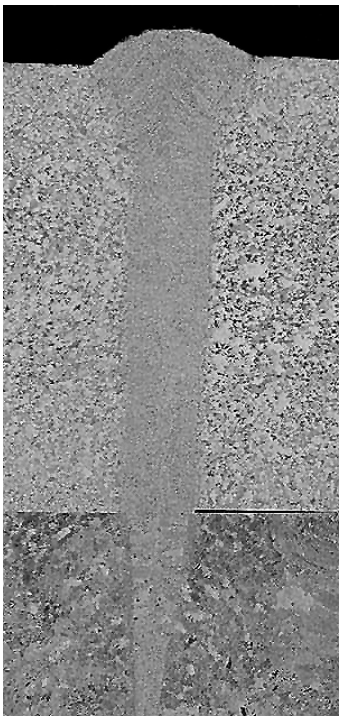

(b)

Figure 13. Defect-free EB weld produced between 12.5 mm thick Ti-48Al-2Cr-2Nb investment cast + HIP'ed + heat-treated plates, preheat of 650^{o}C: (a) top surface; (b) cross-section [39,40].

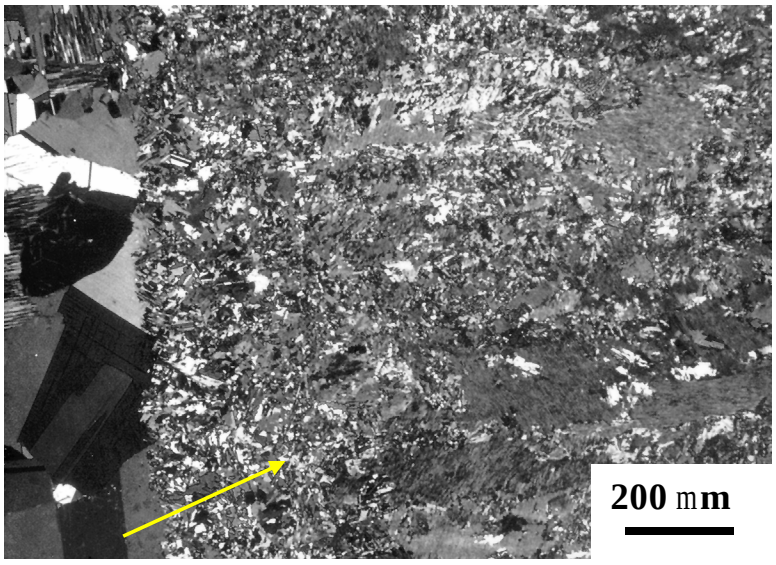

(a)

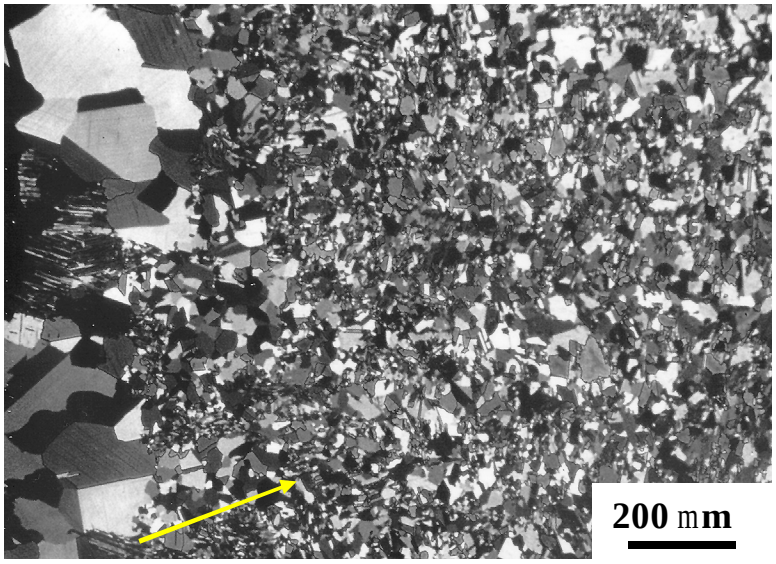

(b)

Figure 14. Polarized light micrographs of postweld stress-relieved (980°C/2hrs) EB weld fusion boundary region in investment cast + HIP'ed + heat-treated plate: (a) Ti-46.3Al-2Cr-2Nb and (b) Ti-48.3Al-2Cr-2Nb plate. Arrows indicate approximate location of fusion line [40].

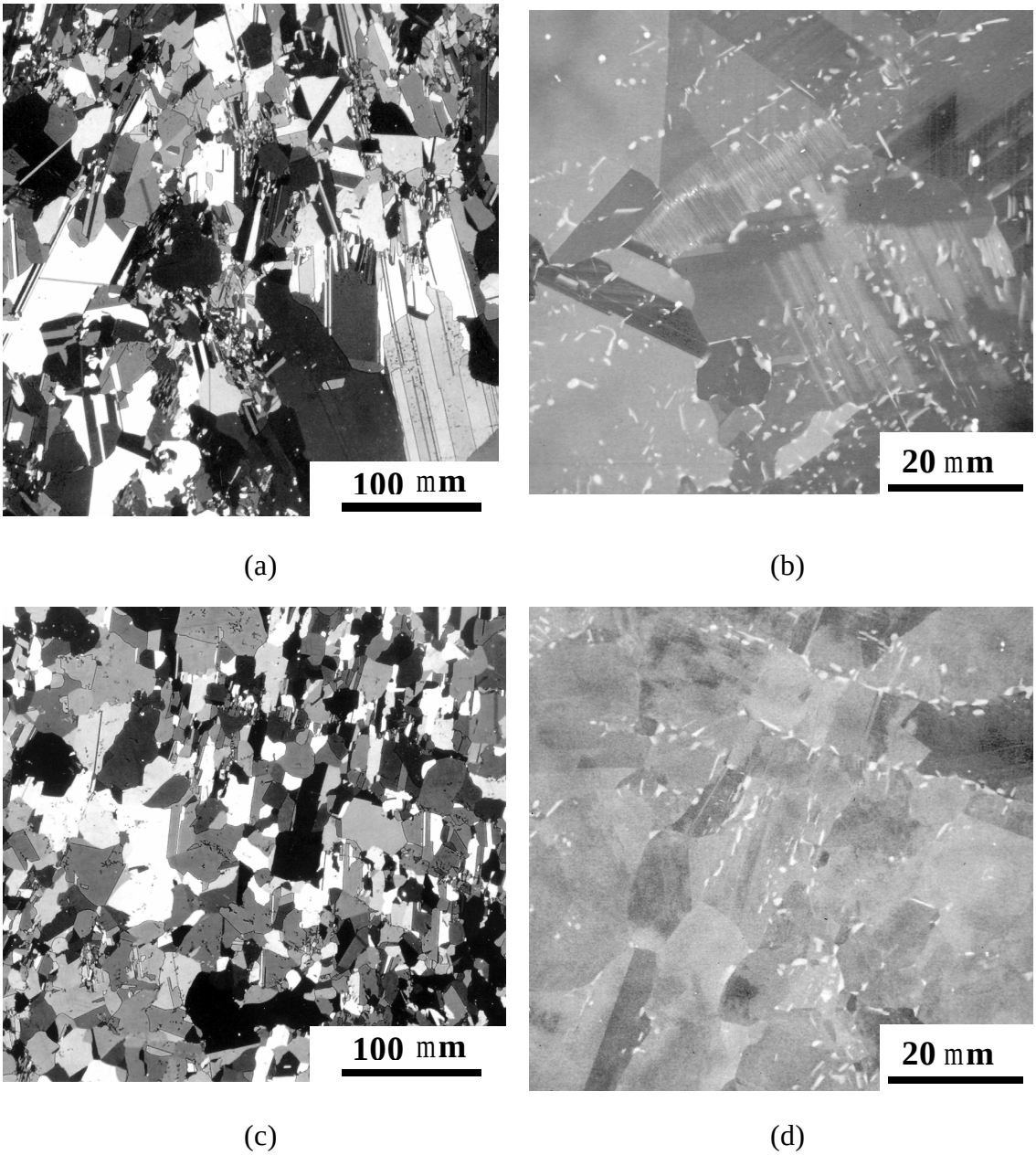

Figure 15. Polarized light (a,c) and SEM/BSE (b,d) micrographs of stress-relieved (980°C/2hrs) and heat-treated (1050°C/5hrs) EB weld fusion zones in Ti-46.3Al-2Cr-2Nb (a,b) and Ti-48.3Al-2Cr-2Nb (c,d) investment cast + HIP'ed + heat-treated plates [40].

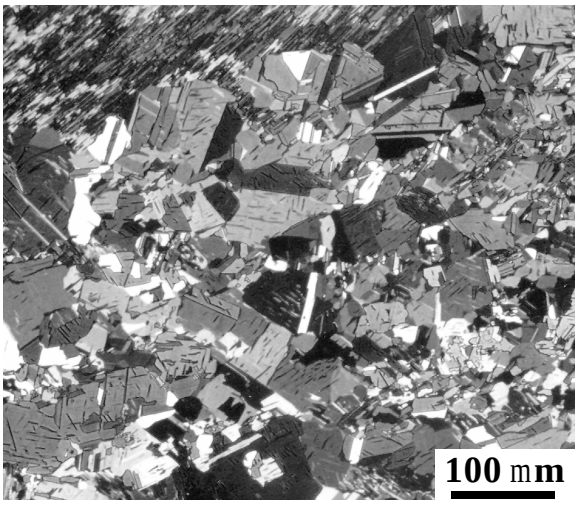

(a)

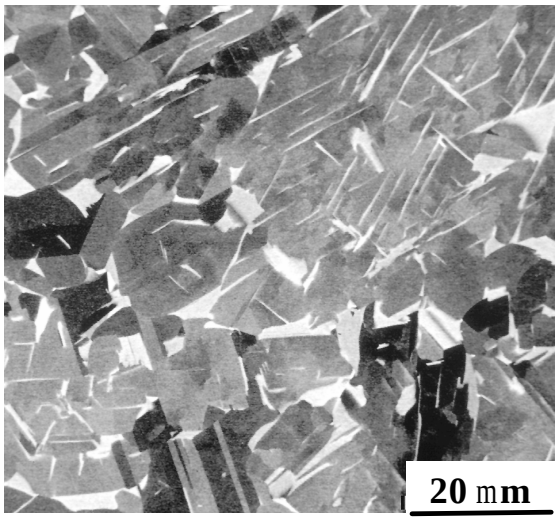

(b)

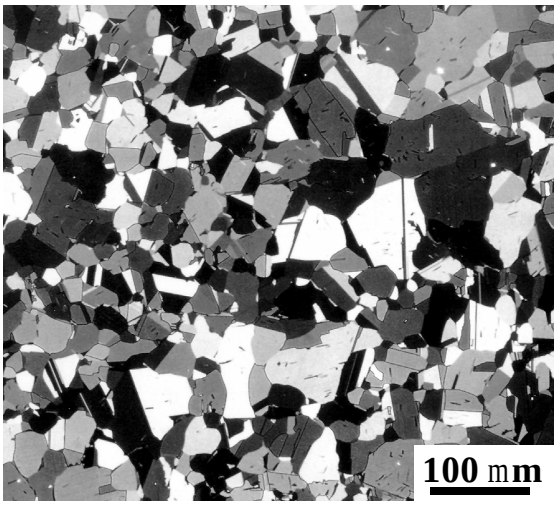

(c)

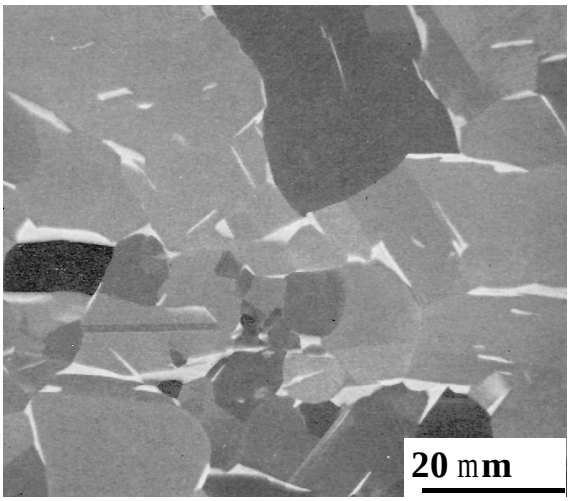

(d)

Figure 16. Polarized light (a,c) and SEM/BSE (b,d) micrographs of stress-relieved (980°C/2hrs) and heat-treated (1250°C/5hrs) EB weld fusion zones in Ti-46.3Al-2Cr-2Nb (a,b) and Ti-48.3Al-2Cr-2Nb (c,d) investment cast + HIP'ed + heat-treated plates [40].

welds. Figure 17 shows tensile properties for fusion zone specimens postweld heat treated at selected conditions, and indicates a general reduction in yield and tensile strength with heat treatment relative to the stress-relieved conditions, but a significant increase in ductility. Conversely, postweld heat treatment generally reduced the fracture toughness of the EB weld fusion zones, with fracture toughness decreasing with an increase in postweld heat treatment temperature and Al content (Fig. 18). A slight increase in toughness of the 1250^{o}C versus the 1150^{o}C heat treatments may have resulted from the secondary precipitation of alpha-two phase within the grains. Mechanical properties observed were consistent with microstructural transitions associated with increased postweld heat treatment temperature and increased Al content (ie., increased recrystallization). Fracture behavior of the welds revealed a mixture of transgranular cleavage fracture through the equiaxed gamma grains, and translamellar fracture.

Laser beam welding offers many of the advantages of EBW, but without the requirement that welding be performed in a vacuum chamber. A primary limitation of LBW relative to EBW is its lower penetration capability, which is dependent upon the laser power and practically restricted to approximately 12.5 mm in titanium plate materials. An early study performed by Threadgill and Baeslack [41] at TWI investigated the CO_2 laser welding of wrought Ti-48Al-2Cr-2Nb. Welds exhibited appreciable solid-state cracking, which was consistent with the high weld cooling rates experienced and the hard, brittle weld zone microstructure.

Shinoda and co-workers [42] utilized a CO_2 laser to produce bead-on-plate laser welds in a 9 mm thick Ti-49Al plate that was sectioned from a casting. Welds produced at a laser power of 1.8 kW and over a range of beam traversing rates from 0.5-2.0 m/min

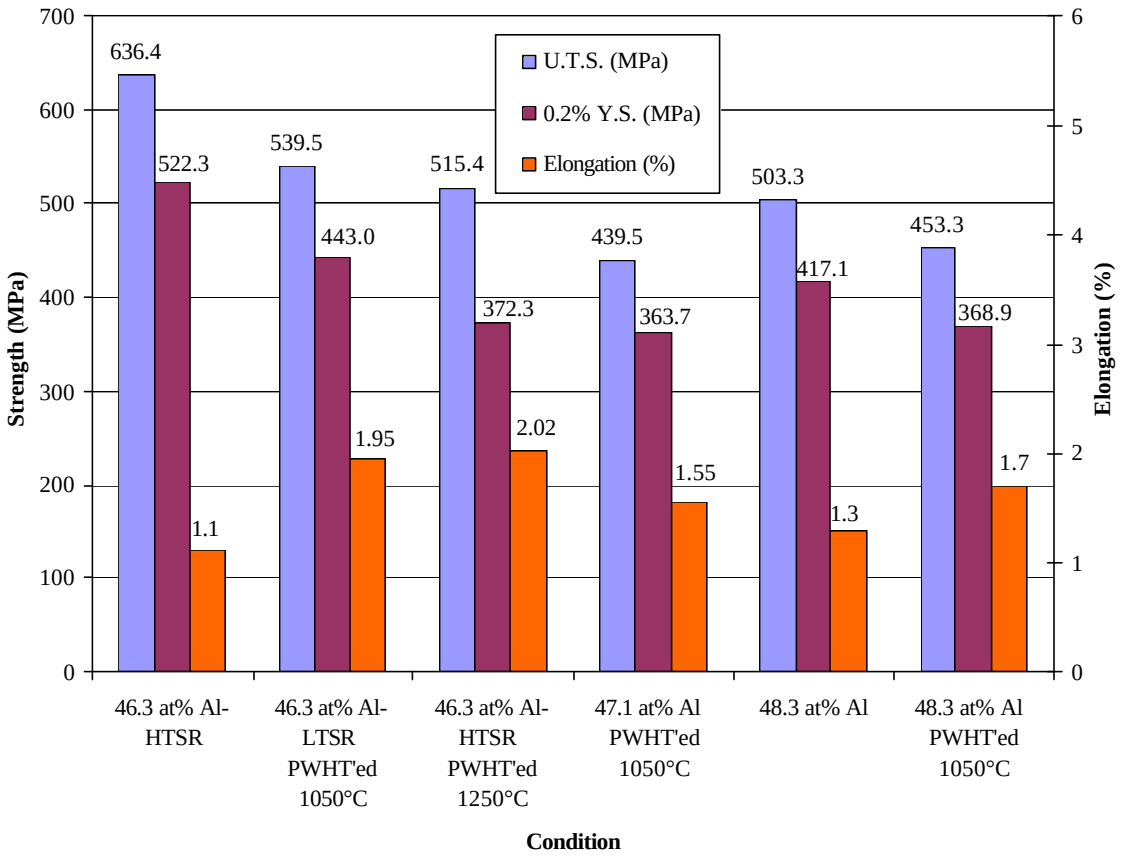

Figure 17. Effects of Al content and postweld heat treatment on the fusion zone tensile properties of EB welds in investment cast + HIP'ed heat-treated Ti-48Al-2Cr-2Nb. HTSR – high temperature stress relief heat treatment (980°C/2 hr), LTSR – low temperature stress relief heat treatment 900°C/2 hr) [40].

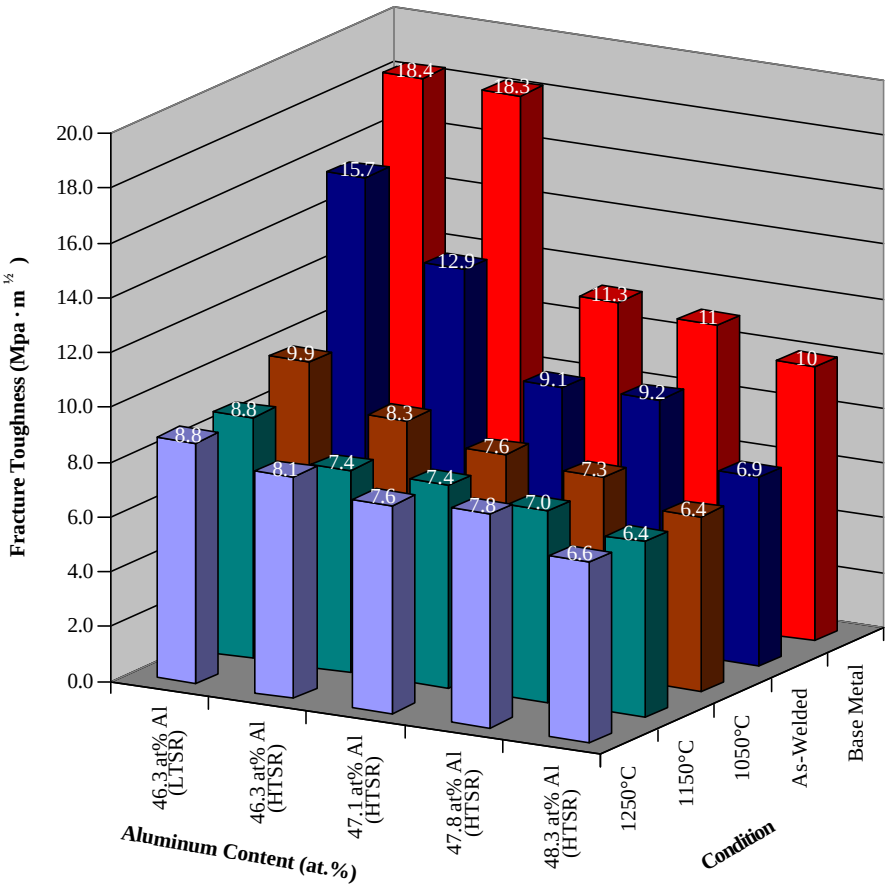

Figure 18. Effects of Al content and postweld heat treatment on the fusion zone fracture toughness of EB welds in investment cast + HIP'ed + heat-treated Ti-48Al-2Cr-2Nb [40].

exhibited extensive cracking in the fusion zone, HAZ and base metal. Cracking was observed to occur both during welding and on cooling to room temperature. The authors suggest that both solidification and solid-state cracking occur, although evidence of solidification cracking was not presented. DPH hardness testing of the laser weld produced at a welding speed of 1 mm/min showed high hardnesses at the fusion zone surface and in the HAZ exceeding 500 DPH versus a base metal hardness of 330 DPH. Although detailed microstructure analysis was not performed in this study, it is suggested that the extremely rapid cooling rates promoted the retention of appreciable alpha-two phase, which is known to embrittle the alloy and promote solid-state cracking.

Lee and co-workers [43,44] investigated the CO_2 laser welding of 50 mm thick coupons sectioned from investment cast + HIP'ed + heat-treated Ti-48Al-2Cr-2Nb plates with Al contents ranging from 45.5 to 50.6 at%. Autogenous welds were produced in an argon-purged chamber that utilized quartz lamps to provide preheat temperatures of up to 600^{o}C. Using different combinations of laser power (1.2-2.0 kW), beam traversing rate (3.4-19 mm/s) and preheat (RT-600^{o}C), they systematically achieved a range of weld cooling rates from approximately 5,000 to 100^{o}C/s (calculated average between 1550^{o}C and 800^{o}C).

Laser beam welds produced at high beam traversing rates and low preheat temperatures exhibited high depth-to-width ratios and partial penetration. Welds produced at higher energy inputs achieved full penetration, but exhibited depth-to-width ratios approaching unity. Welds produced at the higher heat inputs, and at higher Al contents, exhibited occasional solidification cracking along the weld centerline where

columnar grains impinged. SEM analysis of the crack surfaces confirmed their supersolidus origin (Fig. 19).

A primary purpose of Lee's work was to investigate the solid-state cracking behavior of Ti-48Al-2Cr-2Nb, and in particular to establish the relationships between Al content, preheat, weld energy input, and cracking susceptibility. As previously described for EB welds, cracking typically occurs transverse to the weld zone, spaced nearly equidistantly along the length of the weld. As shown by comparing Figs. 20a and 20b for 45.5% and 47.9% Al alloys, respectively, cracking susceptibility increased with a decrease in preheating temperature or laser welding heat input, and with a decrease in Al content. Figure 21 shows a general process parameter window for laser welds produced in the Ti-48Al-2Cr-2Nb alloy. As shown, an increase in Al content resulted in a shift of the curves to the left, i.e., a reduction in solid-state cracking susceptibility, but an increase in solidification cracking susceptibility.

Lee used light and SEM/BSE microscopy to characterize the LB weld solidification characteristics. Based on the dendrite morphologies observed in shrinkage cavities and through BSE imaging of polished specimens, his analysis suggested primary BCC solidification at low cooling/solidification rates and low Al contents, and a transition to HCP solidification at higher cooling/solidification rates and higher Al contents. Light microscopy, SEM and TEM were performed on 45.5, 46.9 and 47.9 at% Al alloys at cooling rates of approximately 5000, 450 and 150^{o}C/s. The most rapidly cooled weld fusion zone in low-Al alloys exhibited primarily retained alpha-two microstructures, with occasional thin gamma platelets (Fig. 22a). At the intermediate

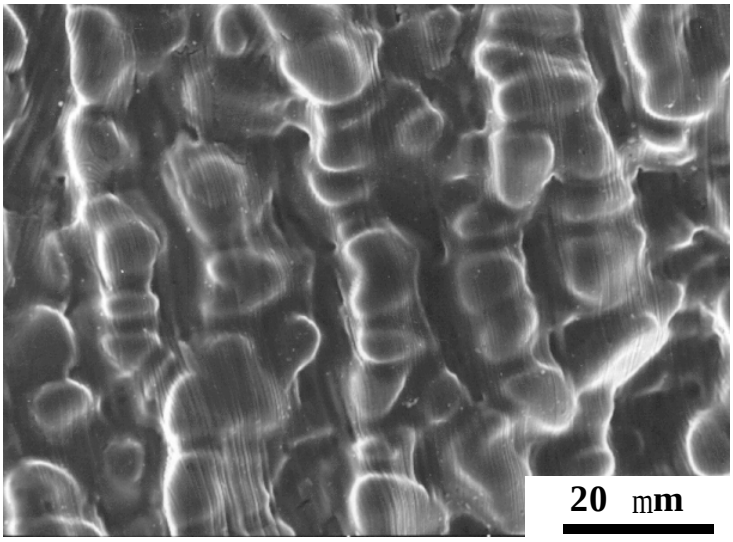

Figure 19. SEM fractograph of solidification crack surface in CO_2 laser weld produced in Ti-46.2Al-2Cr-2Nb (2.0 kW, 3.4 mm/s) [43].

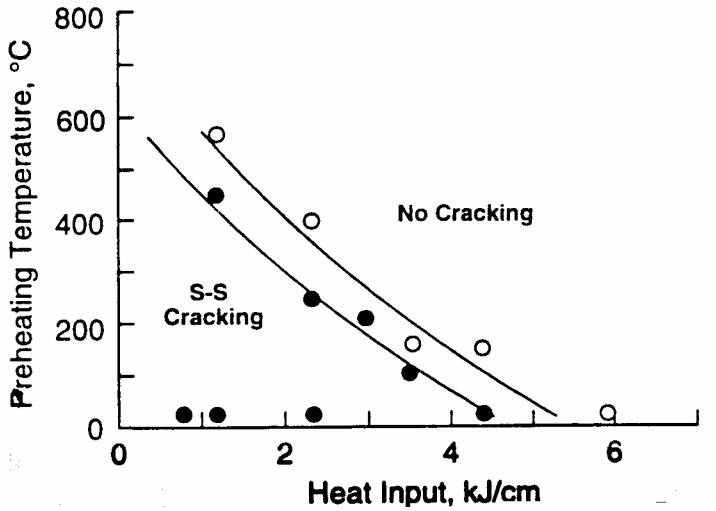

(a)

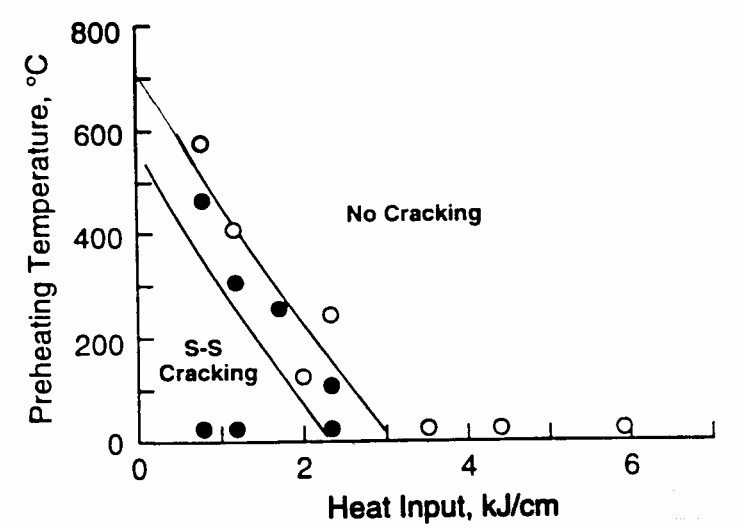

(b)

Figure 20. Effects of preheating temperature and weld heat input on solid-state cracking susceptibility of CO_2 laser welds in (a) Ti-45.5Al-2Cr-2Nb and (b) Ti-47.9Al-2Cr-2Nb alloys [43].

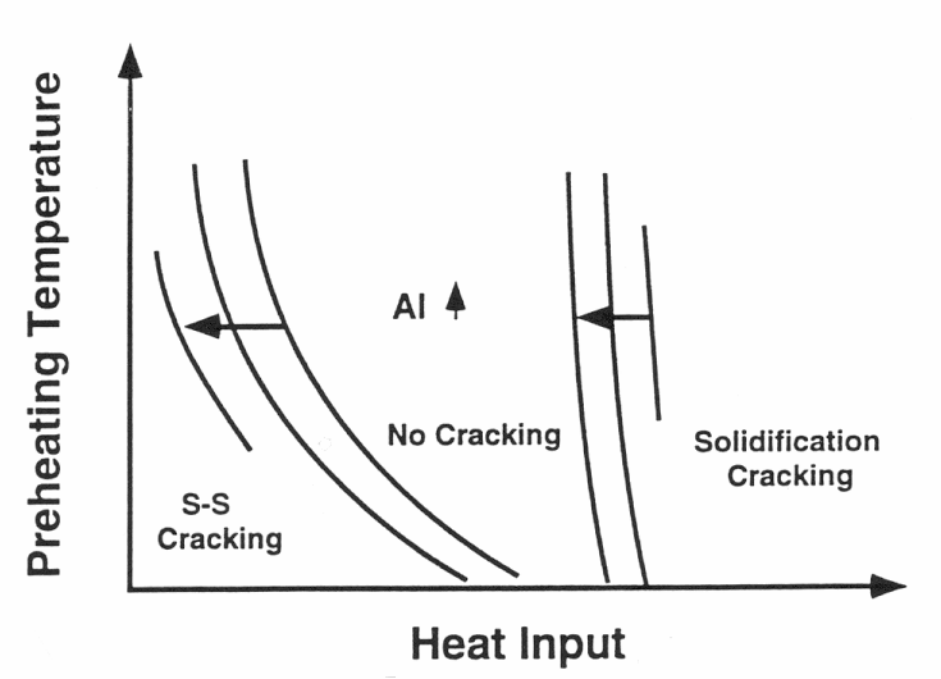

Figure 21. Schematic illustration showing effect of Al content, preheating temperature and weld heat input on susceptibility of CO_2 laser welds in Ti-48Al-2Cr-2Nb to solid-state and solidification cracking [43].

cooling rates, microstructures were comprised of blocky gamma phase (interdendritic or massive), a fine lamellar structure, and a small quantity of retained alpha-two phase. At the slowest rates, the microstructures were predominantly lamellar constituent with some equiaxed gamma grains (Fig. 22b). Higher Al contents promoted more rapid transformation to the lamellar structure (i.e., the critical cooling rate for the formation of the lamellar structure increased with increasing Al content). As shown in Fig. 23, a decrease in cooling rate promoted a decrease in coarseness of the lamellar constituent. Fusion zones and HAZ's of the welds were appreciably harder than the base material (DPH 450-525 versus DPH 225-275). Despite significant microstructural differences, the hardness of the fusion zone decreased only slightly as the Al content increased (for a constant cooling rate) or as the cooling rate decreased (for a constant Al content).

PWHT of the laser welds at 1300^{o}C/10 hrs showed a significant influence of the original solidification structure on the heat-treated microstructure. The microstructures exhibited a combination of equaixed gamma grains and lamellar regions with the gamma grains associated with original interdendritic regions and/or gamma segregate at dendrite boundaries. As shown in Fig. 24, an increase in Al content promoted an increase in the proportion of equiaxed gamma grains versus lamellar constituent and the total volume fraction of gamma phase. For a constant Al content, a decrease in weld cooling rate promoted an increase in the overall microstructural coarseness. PWHT promoted appreciable microstructural softening, reducing fusion zone hardnesses to approximately base metal levels. An increase in Al content promoted a reduction in hardness presumably due to a decrease in the volume % of lamellar alpha-two + gamma constituent.

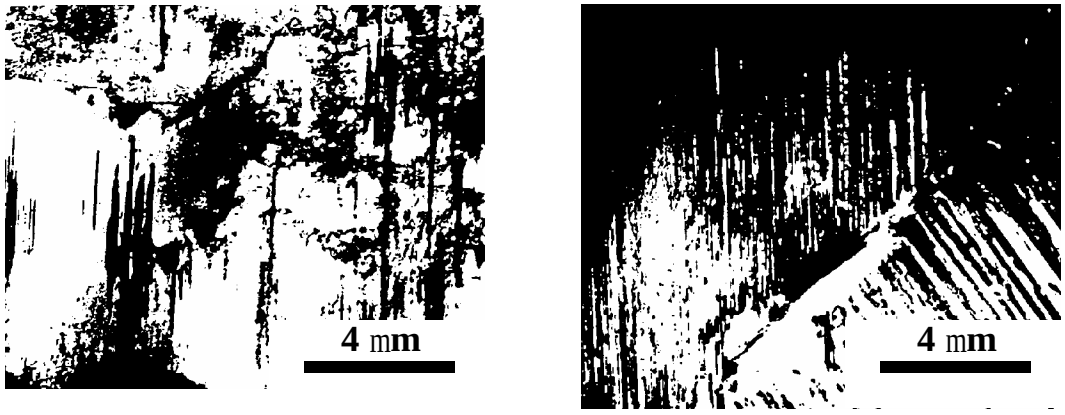

(a) (b)

Figure 22. TEM bright-field micrographs of weld fusion zones in CO_2 laser welded Ti-45.5Al-2Cr-2Nb: (a) 1.5KW, 12.7 mm/s, featureless areas are alpha-two phase; (b) 1.5KW, 3.4mm/s [43].

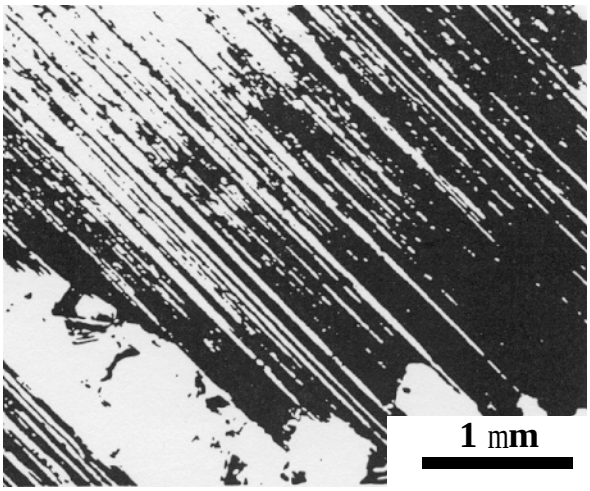

(a)

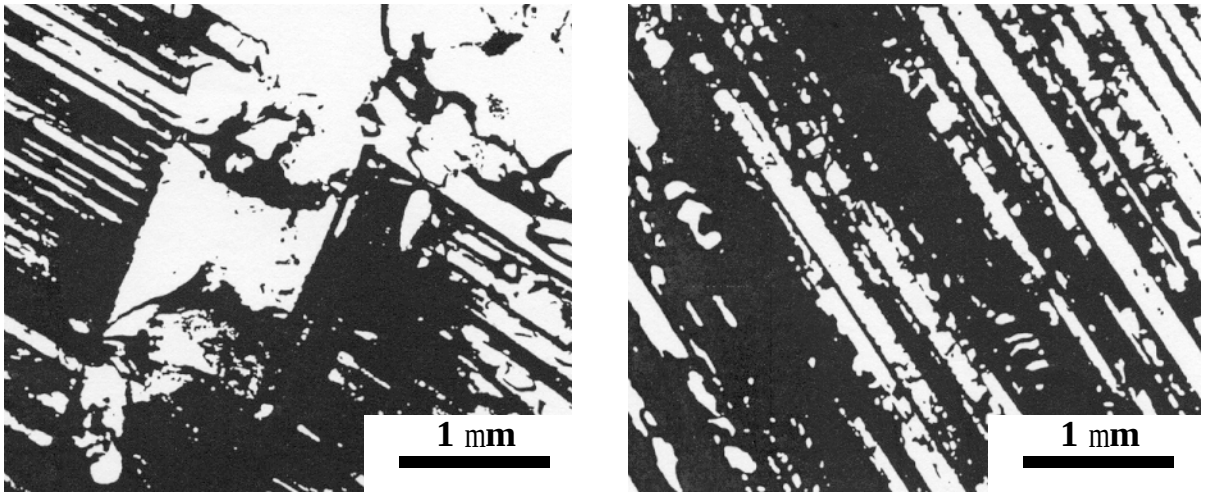

(b) (c)

Figure 23. TEM bright-field micrographs of weld fusion zones in CO_2 laser welded Ti-47.9Al-2Cr-2Nb: (a) 1.5kW, 19 mm/s; (b) 1.5kW, 12.7 mm/s; (c) 1.5kW, 3.4 mm/s [43].

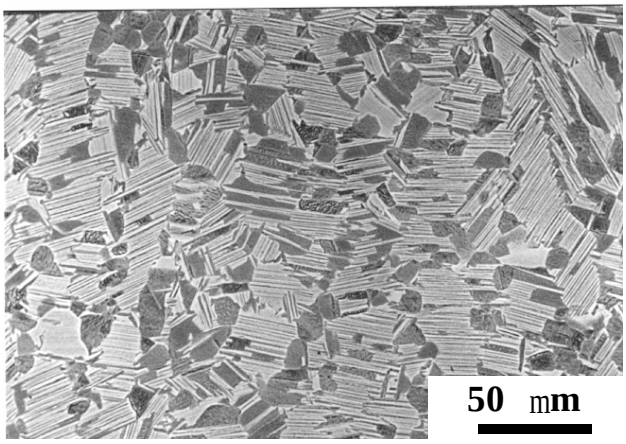

(a)

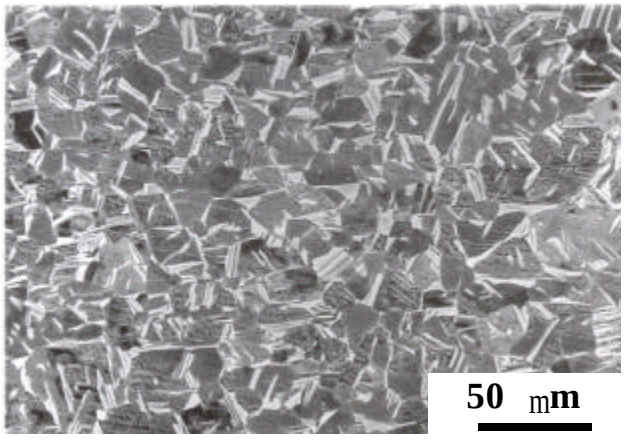

(b)

Figure 24. SEM/BSE micrographs of weld fusion zones in CO_2 laser welded Ti-45.5Al-2Cr-2Nb (a) and Ti-47.9Al2Cr-2Nb (b) postweld heat treated at 1300^{o}C/10 hrs [43].

The CO_2 laser welding of ingot metallurgy Ti-48Al-2Cr sheet was investigated by Klassen et al [45] and Clemens et al. [46]. They noted a strong sensitivity to solid-state cracking during laser welding, but that preheating above the brittle-to-ductile transition temperature allowed the production of crack-free welds on different joint geometries, including overlap, butt and spot welds.

Mallory [47] investigated HAZ microstructure evolution in CO_2 laser welds in Ti-47Al-2Cr-2Nb, Ti-48Al-2Cr-3Nb, and Ti-47-2Cr-3Ta investment cast + HIP'ed + heat-treated castings. Welds produced over a wide range of energy inputs and cooling rates showed far HAZ's to be comprised primary of duplex structures with platelets of alpha-two phase partitioning equiaxed gamma grains. The near-HAZ, which transformed entirely to alpha phase on heating, was comprised of lamellar, Widmanstatten or acicular/feathery gamma phase morphologies with increasing cooling rate. PWHT resulted in near-gamma microstructures, with alpha-two phase at gamma grain boundaries. Mallory also used the Gleeble to develop simulated weld HAZ microstructures over a range of cooling rates.

3.3 Friction Welding

Friction welding is a solid-state welding process that produces coalescence by the frictional heating of two parts under an applied load. This welding process is generally associated with interfacial heating to near-solidus temperatures, and the application of a forging force that squeezes highly-plasticized metal out of the joint interface, thereby promoting final welding between clean, nacient surfaces. Several variants of friction welding have been developed and are currently being utilized to join gamma titanium aluminides, including inertia-friction welding, continuous-drive friction welding, linear-

friction welding and, most recently, friction-stir welding.

An early study by Hou et al. [48] examined the microstructure of an inertia-friction weld produced by GE Aircraft Engines in wrought Ti-48Al-2Cr-2Nb that exhibited a duplex base metal microstructure comprised of heavily twinned gamma grains and occasional colonies of lamellar alpha-two + gamma constituent. The center of the weld heat-and-deformation zone (HDZ) exhibited a lamellar constituent with extremely fine, equiaxed gamma grains located primarily at colony boundaries, while the outer HDZ exhibited extensive twinning of coarser gamma grains and partial recrystallization. Cr-rich B2 phase was observed in the base metal and the HDZ. Cracking was observed to occur in the HDZ, particularly along grain boundaries and colony boundaries in the outer HDZ, suggesting its occurrence at elevated temperatures during the welding process.

English and Vasudevan [49] characterized the microstructure and mechanical properties of inertia-friction welds produced in isothermally-forged and heat-treated Ti-48Al-2Cr-2Nb bars. Although welds produced at high axial loads promoted wedge cracking along grain boundaries, particularly in the highly-deformed regions of the outer-HDZ, the application of optimized welding parameters using low applied axial loads and a high weld energy input, and which promoted shallower thermal gradients across the weld, generated welds that exhibited satisfactory interfacial upset and that were free of cracking. The heat-treated base metal microstructure varied from duplex to near-gamma and contained a wide range of gamma grain sizes with occasional colonies of distorted lamellar constituent. The hourglass-shaped inner-HDZ exhibited a fine, recrystallized

gamma grain structure (2-3 microns average diameter), with occasional regions of fine lamellar constituent. The unrecrystallized outer-HDZ exhibited an increase in the volume of alpha-two at gamma grain boundaries relative to the heat-treated base metal microstructure. PWHT at 1300^{o}C/10 hr promoted an increase in the gamma grain size in the inner-HDZ (10-30 microns), the proportion of lamellar constituent in all regions, and in the volume fraction of alpha-two at gamma grain boundaries both in the inner and outer HDZ's.

Knoop microhardness traverses across the weld zone showed a significant increase at the inner HDZ, to over KHN 400, versus a base metal hardness of about KHN 250. Significant grain coarsening associated with postweld heat treatment reduced hardnesses across the HDZ to base metal levels. Consistent with hardness results, tensile testing of the as-welded and postweld heat-treated specimens showed failure to occur in the base material, with appreciable scatter in % elongation at fracture from 0 to 1.5%. Fracture toughness testing of the inner-HDZ showed as-welded toughness to average approximately 6.6 MPa-m$^{1/2}$, with postweld heat treatment increasing toughness to an average of 10.5 MPa-m$^{1/2}$, which was somewhat below that of the parent material (11-16.5 MPa-m$^{1/2}$). Fracture of the tensile and fracture toughness specimens occurred by cleavage across equiaxed gamma grains, with little evidence of intergranular fracture, and with some evidence of interlameller splitting in postweld heat-treated specimens.

Zhang and co-workers [50] investigated microstructure evolution during the IFW of investment cast + HIP'ed + heat-treated Ti-47.3Al-2.0Cr-1.9Nb. Inertia-friction welds were produced by GE Aircraft Engines between 25.4 mm diameter rod that exhibited a

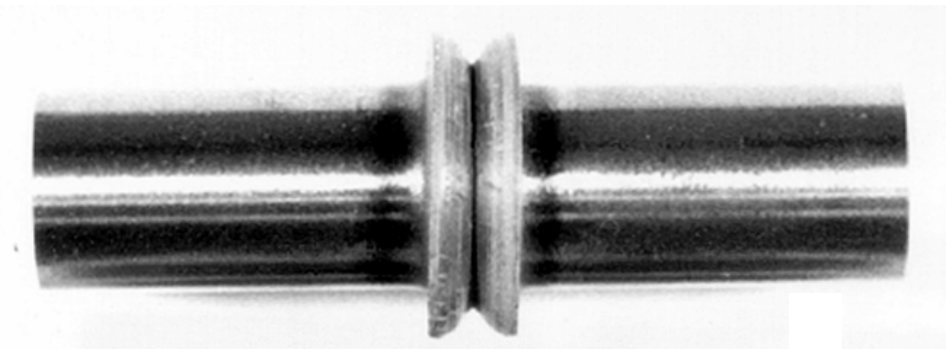

(a)

(b)

Figure 25. Inertia-friction weld in investment cast + HIP'ed + heat-treated Ti-48Al-2Cr-2Nb: (a) welded rod; (b) light macrograph of weld zone through axial centerline [50].

microstructure comprised of approximately 50 volume % equiaxed gamma grains and 50% lamellar alpha-two + gamma constituent. As shown in Fig. 25, the use of optimized welding parameters resulted in uniform expulsion surrounding the cylindrical weldment, and an absence of lack-of-bonding defects or cracking in the weld.

Detailed characterization of the weld HDZ showed a microstructure appreciably refined relative to the base metal. The interface exhibited small colonies (40 um in diameter) of very fine lamellar alpha-two + gamma constituent (Fig. 26), suggesting that this region experienced temperatures well into the alpha phase field, was dynamically recrystallized, and then rapidly cooled at approximately 100 to 200^{o}C/s. The inner-HDZ also contained bands oriented parallel to the interface that were enriched in Al and depleted in Ti relative to the base metal, and which exhibited small equiaxed gamma grains and lamellar constituent. The outer-HDZ of the welds exhibited a high dislocation density, and severely deformed lamellar colonies, presumably that existed in the base metal microstructure prior to welding. Differences between the weld interface microstructures and those observed by Hou et al. (Widmanstatten gamma) and English (fine, equiaxed gamma grains), can be attributed to variations in welding parameters that promoted a lower strain level, and higher peak temperature at the weld interface than used previously.

As observed by previous investigators, Zhang et al. found that postweld heat treatment promoted appreciable recrystallization of the lamellar microstructure to equiaxed gamma, with alpha-two located at grain boundaries and as acicular platelets within the gamma grains (Fig. 27). Interestingly, the banded regions transformed to very coarse gamma grains with negligible evidence of alpha-two either within the grains, or at

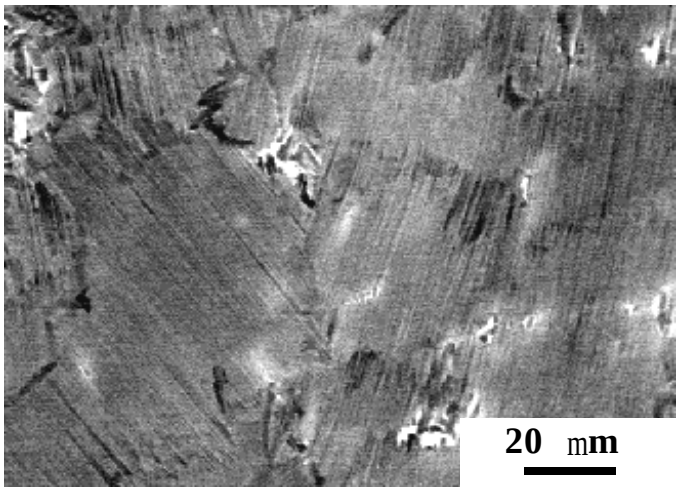

(a)

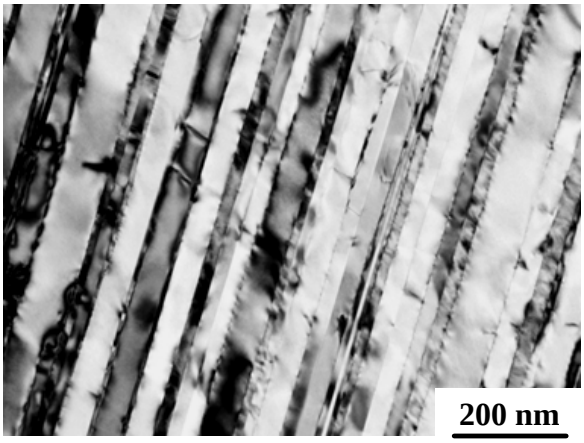

(b)

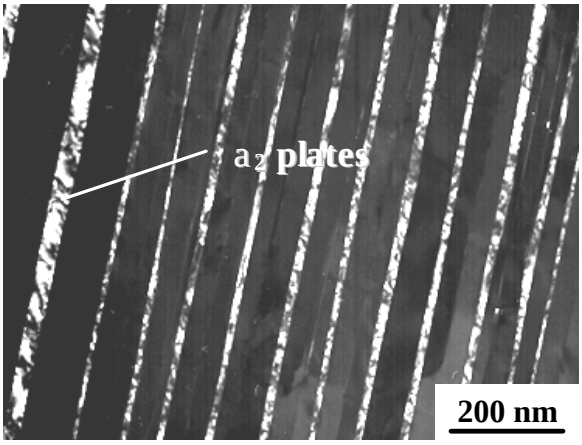

(c)

Figure 26. Inner heat-and-deformation zone of inertia-friction weld in cast + HIP'ed + heat-treated Ti-48Al-2Cr-2Nb[50]: (a) SEM/BSE image; (b) TEM bright-field micrograph; (c) TEM dark-field micrograph.

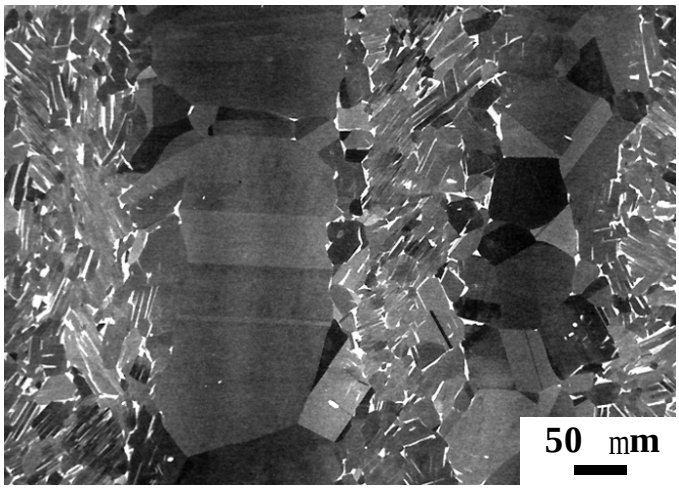

(a)

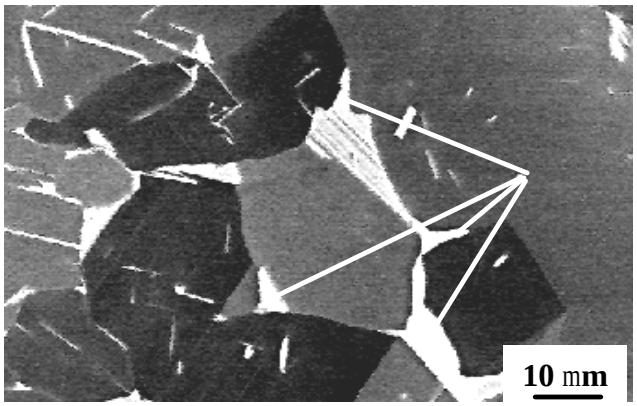

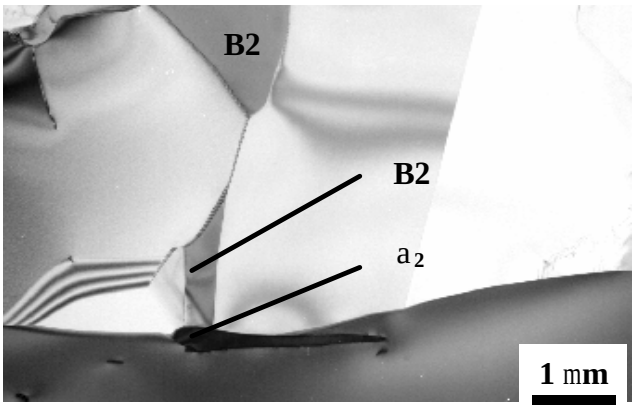

(b) (c)

Figure 27. Inner heat-and-deformation zone of inertia-friction weld in cast + HIP'ed + heat-treated Ti-48Al-2Cr-2Nb after PWHT at 1250°C/4 hr [50]: (a) SEM/BSE image; (b) TEM bright-field micrograph; (c) TEM dark field micrograph.

grain boundaries, which is consistent with their general enrichment in Al. It is of interest to note that as in the EB welds [40], PWHT at 1250^{o}C promoted the formation of B2 at gamma grain boundary triple points (Fig. 27c). Microhardness testing across the weld zone indicated appreciable hardening in the as-welded inner-HDZ (DPH 400), but that PWHT promoted softening to levels comparable to that of the unaffected base metal (DPH 250).

An early study by Horn [51] examined the continuous-drive friction welding of a Ti-48-50Al gamma titanium aluminide that exhibited a completely lamellar alpha-two/gamma microstructure. Significant microstructural refinement at the weld interface was found to promote an increase in hardness from DPH 360 in the base metal to over DPH 500 at the weld interface.

Shinoda and co-workers [42] used continuous-drive friction welding to join 15 mm diameter cast bars of Ti-49Al–1Mn. Through the optimization of welding forge pressure and time, they were successful in producing high integrity, defect-free welds. They noted a weld interface region microstructure that was appreciably refined relative to the coarse lamellar microstructure in the base metal. Thermal exposure at 700, 800 and 900^{o}C for 30 minutes promoted coarsening of the weld zone microstructure and no change in the base metal microstructure. Hardness analysis of the welds showed an increase from approximately DPH 330 in the base metal to over DPH 400 at the weld interface, and an increase in peak hardness with a decrease in weld time. Tensile testing of the weld joints at room and elevated temperatures to 900^{o}C determined the weld region to generally be stronger than the base metal, with base metal failure occurring exclusively in the base metal except for welds produced at 10 seconds and tested at 900^{o}C. These

tensile results are consistent with the more refined microstructure and higher hardness exhibited by the weld zone relative to the base metal.

Hurta et al. [24] utilized continuous-drive friction welding to join exhaust valve stems to disks in Ti-48Al-2Cr, Ti-46Al-1.5Cr-0.9Nb-0.1Si, and Ti-48Al-2Cr-2Nb alloys, including both similar and dissimilar alloy joints between these alloys. They observed appreciable microstructural refinement in the weld zone and a corresponding increase in hardness from approximately DPH 350 to DPH 500.

Linear-friction welding of gamma titanium aluminides has been studied at TWI in collaboration with The Ohio State University. Relative to conventional IFW and CDFW, LFW provides a capability to join non-axi-symmetric components, such as rectangular shapes. Early studies at TWI by Baeslack and co-workers [52] examined the LFW of wrought Ti-48Al-2Cr-2Nb to itself, and dissimilar welds to Ti-24Al-11Nb alpha-two titanium aluminide. The welds exhibited HDZ grain refinement, but also appreciable solid-state cracking. Subsequent work by Threadgill and co-workers [53] at TWI on wrought Ti-48.7Al-2.0Cr-1.9Nb and cast Ti-48Al-2Mn-2Nb performed a parametric study to determine the influence of welding parameters on weld integrity and microstructure. In the wrought alloy, they found that the application of a high forging force promoted appreciable recrystallization at the weld interface and a fine, equiaxed gamma grain structure, while a lower forge force promoted transformation to a lamellar alpha-two/gamma microstructure. Although this transition may be attributed to differences in the weld thermal-mechanical conditions experienced during welding, they further suggest an influence of oxygen contamination in promoting transformation to the lamellar structure. The application of a higher forge force promoted greater expulsion of

contaminated metal from the weld interface. Unfortunately, the application of a higher forge force, and the associated higher cooling rates and greater weld stresses, promoted a greater susceptibility to solid-state weld cracking, suggesting the requirement for inert-gas shielding of the welding process.

Characterization by Threadgill and co-workers [53] of welds produced in a cast Ti-48Al-2Mn-2Nb alloy that exhibited a lamellar base metal microstructure revealed an interface microstructure comprised of non-parallel laths at original dendrite cores, and regions of parallel lamellae at interdendritic regions. In the outer-HDZ they noted appreciable deformation twinning of gamma phase in the lamellar base metal constituent.

Baeslack and co-workers [54] performed more in-depth characterization of linear-friction welds produced by TWI in the wrought Ti-48.7Al-2.Cr-1.9Nb (Fig. 28). In the outer-HDZ, equiaxed gamma grains in the duplex base metal partially transformed to alpha-two phase by the rapid growth of acicular plates of alpha phase across equiaxed grains, as has been observed previously in GTA weld HAZ's. At the weld interface, where the microstructure had completely transformed to alpha-two phase on heating, the microstructure was comprised of small colonies of lamellar alpha-two + gamma constituent, indicating dynamic recrystallization of alpha phase and subsequent decomposition of these grains during weld cooling (Fig. 29). PWHT at 1300^{o}C/10hrs promoted gamma grain recrystallization across the HDZ. Occasional regions of coarse lamellar constituent were observed at the weld interface, particularly near the outer periphery of the weld. As for inertia-friction and continuous-drive friction welds, hardness traverses across the linear-friction welds showed a significant increase near the weld interface (Fig. 30), but appreciable softening following PWHT.

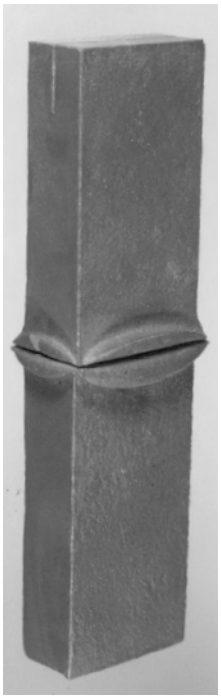

Figure 28. Linear-friction weld in Ti-48Al-2Cr-2Nb [54].

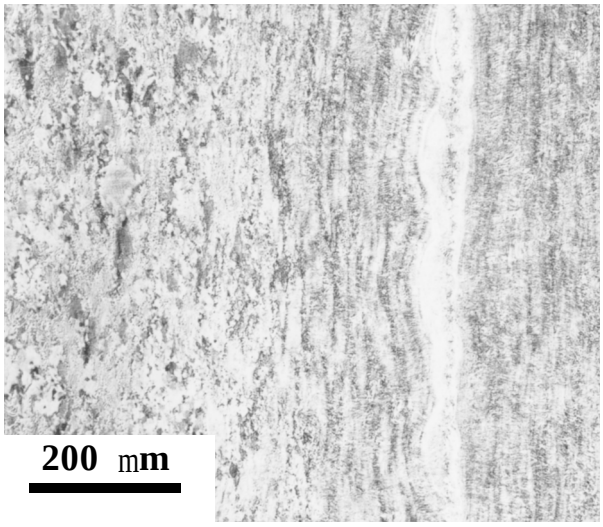

(a)

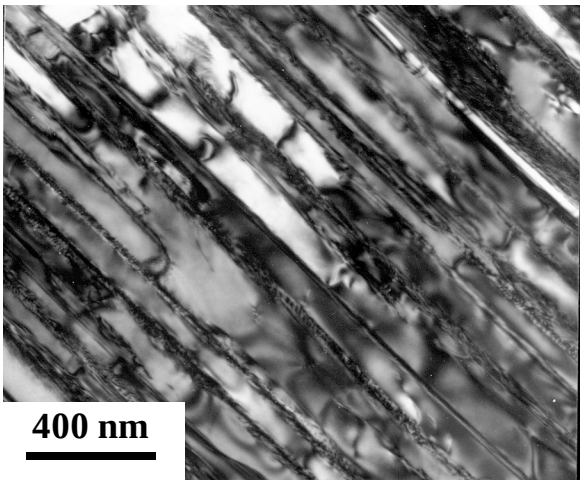

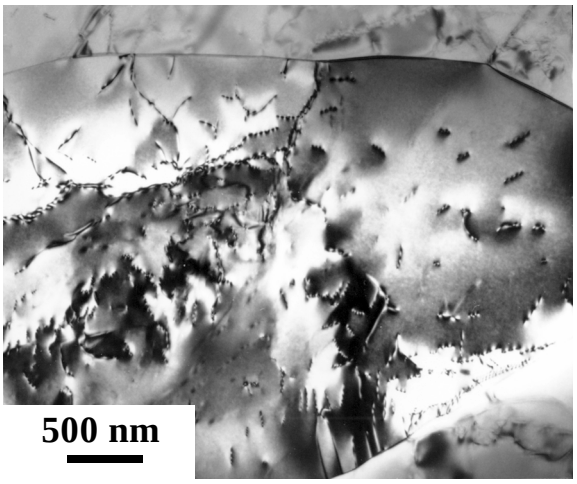

(b) (c)

Figure 29. Heat-and-deformation zone at weld interface for linear-friction weld in Ti-48Al-2Cr-2Nb: (a) light micrograph; (b) ; (c) TEM bright-field micrographs [54].

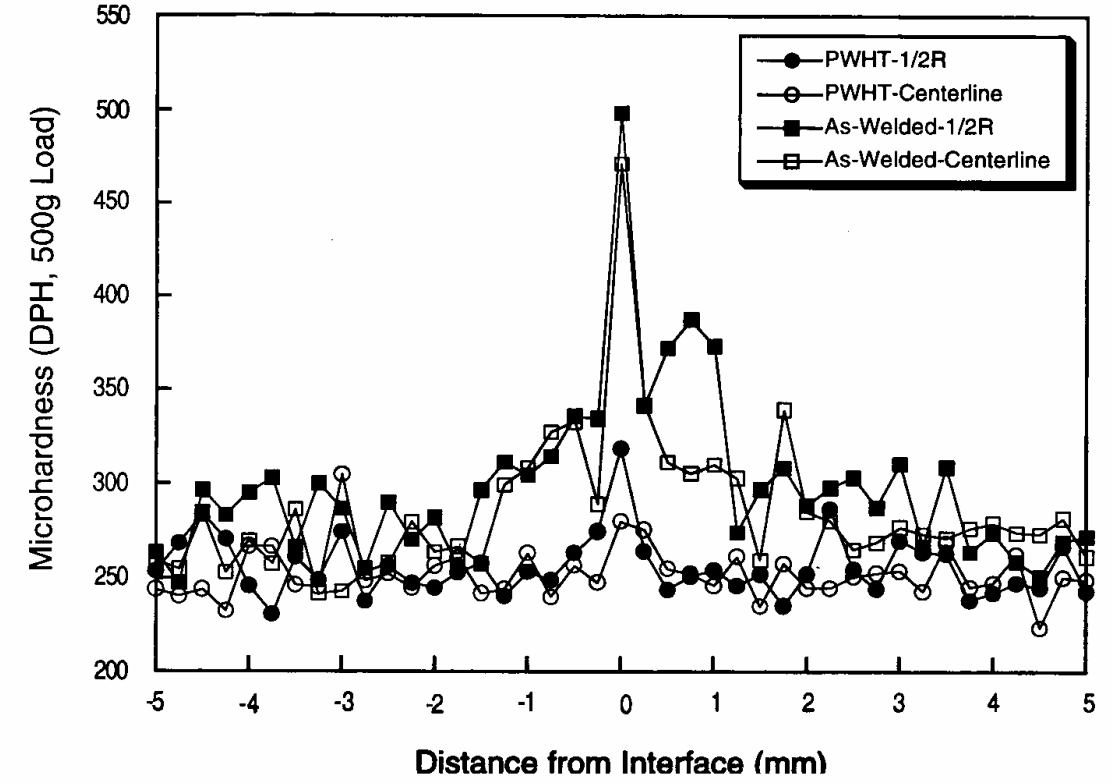

Figure 30. Diamond pyramid hardness traverses across linear-friction welds in cast + HIP'ed + heat-treated Ti-48Al-2Cr-2Nb at weld axial centerline and ½ diameter radius in the as-welded and postweld heat-treated (1300°C/10hrs) conditions [54].

Friction-stir welding is a comparatively new friction welding process in which a rotating, non-consumable pin made of a high-strength material is advanced between two contacting metal plates. The pin, which is attached to a cylindrical shoulder that rotates at several hundred RPM, is plunged into the workpiece at the joint interface, and translated along the length of the joint producing localized frictional heating and themomechanical deformation, thereby generating a high-integrity, solid-state weld. Principal welding parameters include tool design, tool rotation speed, the downward forging force, and the pin tool design. The weld "stir zone" is typically characterized by a fine, recrystallized grain structure and low level of residual work. The process is being widely applied for the joining of aluminum alloys, and recently has been successfully applied to conventional titanium alloys, such as Ti-6Al-4V [55,56]. Although short welds have been produced by TWI on gamma titanium aluminides, the principal difficulty is short tool life, as the high-temperature strength of titanium aluminides, relative to conventional titanium alloys, results in rapid tool wear and deterioration. It is anticipated that new tool materials and designs will eliminate these .

3.4 Diffusion Welding

Diffusion welding is a solid-state joining process in which the interfaces of two workpieces are brought together at elevated temperatures and under a low to moderate force to produce a solid-state weld. During the initial stages of the process, surface asperities impinge and are plastically deformed, thereby exposing clean metallic surfaces. As the process continues, typically from 15 minutes to several hours, welding occurs through a combination of diffusion, recrystallization and ultimately grain boundary migration across the weld interface. Titanium alloys are intrinsically amenable to

diffusion welding because titanium oxide readily dissolves at welding temperatures, and because the yield strength of titanium is low at these temperatures, thereby enhancing plastic deformation. The presence of a tenacious, high-melting point oxide on the surface of aluminum alloys makes the diffusion welding of these materials very difficult. Fortunately, work described below demonstrates that gamma titanium aluminides behave like titanium in their diffusion weldability, despite their high aluminum content.

Early work by Nakao et al. [57,58] investigated the diffusion welding characteristics of an arc-melted Ti-52Al binary alloy. Initially, they examined the influence of welding temperature, pressure and time on the amount of oxide film and the number and size of small voids at the weld interface. Based on this analysis, they determined welding parameters of 1200^{o}C, 15 MPa and approximately 1 hr to be optimum for producing sound weld joints. The tensile testing of joints produced using these parameters found fracture at room temperature to occur in the base metal, but fracture at 800^{o}C and 1000^{o}C to occur along an unrecrystallized, relatively flat weld interface at strength levels below those of the base metal. In order to promote recrystallization of gamma grains at the weld interface, and the migration of this interface, they welded a second set of specimens with surfaces specially prepared using a coarser emery paper that promoted plastic deformation, and welded using a lower pressure of 10 MPa. Tensile testing of these joints showed base metal strengths and fracture away from the weld interface at room temperature and 800^{o}C. Although this recrystallization treatment promoted interface migration and an absence of flat fracture, tensile fracture at 1000^{o}C occurred at the interface at strength levels well below the base metal. Postweld heat treatment at 1300^{o}C was subsequently given to the specimens in

order to promote the growth of recrystallized grains at the weld interface. Tensile fracture of these specimens at 1000^{o}C occurred in the base metal.

Initial diffusion welding studies by Yan and co-workers [59] investigated the influence of welding temperature, pressure and time on weld integrity and shear properties. Consistent with the results of Nakao, they found that the application of temperatures above 1100^{o}C and pressures above 20 MPa promoted room temperature properties comparable to those of the base metal, with failure remote from the weld interface. High-integrity welds were also produced for joints containing sputter-coated interlayers of Ti, Cr, V, Mn, or Nb, however, postweld homogenization heat treatments at temperatures up to 1400^{o}C were required to fully dissolve some interlayers and homogenize the weld region composition, and provide acceptable mechanical properties. Finally, they performed transient liquid phase welding using a Cu interlayer. The formation of highly stable intermetallics during this process is undesirable.

Yan and co-workers [60] subsequently studied the diffusion welding of a binary Ti-48Al alloy. They examined the influence of welding conditions, including temperature, pressure, time and surface condition, on the joint integrity and mechanical properties (shear and bending). Although welds were produced at 900^{o}C and a high pressure of 150 MPa, they observed that welding becomes easier and shear properties improved at welding temperatures of 1100^{o}C and above, and welding pressures of 20 MPa and above. For these higher temperature welding conditions, fine recrystallized gamma grains less than 2 microns in diameter nucleate and grow at the weld interface. They attribute the nucleation of these gamma grains to the deformation of asperity peaks on the rough ground (#1200 grit) mating surfaces during the application of the welding

pressure. This interfacial recrystallization was further shown to improve weld strength by removing planar interface boundaries that characterized diffusion welds produced between polished surfaces. Note that they do not recommend the use of even rougher surface preparations, as the elimination of interfacial voids created during the initial stages of welding via diffusional mechanisms can take a very long time. Welds produced between ground specimens typically failed in four-point bending away from the joint interface at both room and elevated temperatures (600^{o}C). In order to produce high integrity welds without simultaneously applying high temperatures and high pressures, Yan and co-workers demonstrated the use of a two-stage welding process. This process is comprised of a first stage of high pressure (30-40 MPa) at low temperature (1000^{o}C) for a short time, followed by a second stage of low pressure (5 MPa) but higher temperature (1100^{o}C) for a longer time. During the first stage, high plastic strain at the weld interface plastically deforms surface asperities, thereby promoting subsequent recrystallization and an ultimate weld microstructure that promotes optimum mechanical properties. The shear strength of welds produced using this two-stage technique approached 80% of the base material.

Yan and Wallach [60,61] further investigated the solid-state diffusion welding of a Ti-48Al gamma titanium aluminide using sputter-coated interlayers (0.5-1.5 microns in thickness) of Ti, V, Cr, Mn, Nb and Mo. The primary purpose of this approach was to allow for the production of high-integrity welds with a reduction of the welding temperature, pressure and time. In their study, welds were produced using welding parameters of 1000^{o}C, 20 MPa, and 30 minutes. They observed that, for the same welding conditions, weld integrity was superior to that for welds produced with no

interlayer. However, they noted that a significant effect of the interlayer on the microstructure at the weld interface, including interdiffusion zones with Ti, V, Nb and Mo, and multiple diffusion zones and second phases with Cr and Mn. Furthermore, the shear strength in the as-welded condition was typically less than 10% that of the base metal. In order to promote further homogenization of the interlayer into the base metal substrates, a postweld heat treatment of 1340^{o}C/2hrs was given to the welds. For the weld produced with a Nb interlayer, the weld interface appeared comparable to the original base metal microstructure, however, for the Ti, V, Cr, Mn and Mo interlayers, a wide band of lamellar gamma/alpha-two constituent was present at the interface that contained only a few atomic % of the interlayer element. Postweld heat treatment significantly enhanced the weld shear strengths, with the V interlayer weld exhibiting a strength comparable to that of the base material. Bend specimens produced from heat-treated welds using V and Nb interlayers exhibited excellent strength and ductility comparable to that of the base metal, and failed in the base metal at room temperature. At 600^{o}C, the interlayer welds actually exhibited greater strength and ductility than the base metal. However, a detrimental effect of V, Cr and Mn on the oxidation resistance may be expected.

Godfrey et al. [62-64] investigated the diffusion welding of a cast and heat-treated Ti-48Al-2Mn-2Nb alloy, and in particular, the influence of the base metal microstructure (lamellar, duplex and fully gamma) and welding conditions on gamma grain growth at the weld interface. They observed the nucleation of fine (10-20 microns in diameter) twin-related gamma grains at the weld interface that grew primarily away from the interface (Fig. 31), with more rapid grain nucleation and growth for the lamellar and

duplex microstructures for welding in a temperature range of 1200-1350^{o}C for 15 and 45 minutes, using a 10 MPa load and 1200 grit SiC paper surface preparation. They also noted an increase in the volume fraction of alpha-two phase near the weld interface, which they attributed to oxygen enrichment in this region. The welding thermal excursion did not significantly impact the base metal grain size for the fully gamma and duplex specimens, although the precipitation of Widmanstatten alpha-two was observed in gamma grains for specimens welded at high temperature. For the lamellar and duplex microstructure specimens, coarsening and/or decomposition of the lamellae, and the formation of allotriomorphic gamma was observed especially for specimens welded at 1250^{o}C.

Cam et. al. [7,65-67] investigated the diffusion welding of both cast and rolled Ti-Al. They found the optimum welding parameters for the cast product to be 1200^{o}C and 20 MPa, and for the rolled product to be 1000^{o}C and 20 MPa. As with previous investigators, the observed recrystallized gamma grains at the weld interface. They also observed that the strength of welds produced at lower temperatures could be enhanced through postweld heat treatment.

Glatz and Clemens [68] investigated the diffusion welding of a Ti-47Al-2Cr-0.2Si sheet material in regard to potential superplastic forming/diffusion welding operations. Welding at a temperature of 1000^{o}C, a pressure of 20-40 MPa, and times of 1-3 hrs produced high integrity welds with base metal tensile properties.

Holmquist and co-workers [69-71] examined the diffusion welding of Ti-6Al-4V (wt%) and Ti-5.8Al-4.0Sn-3.5Zn-0.7Nb-0.5Mo-0.35Si-0.06C (IMI 834) (wt%) to a

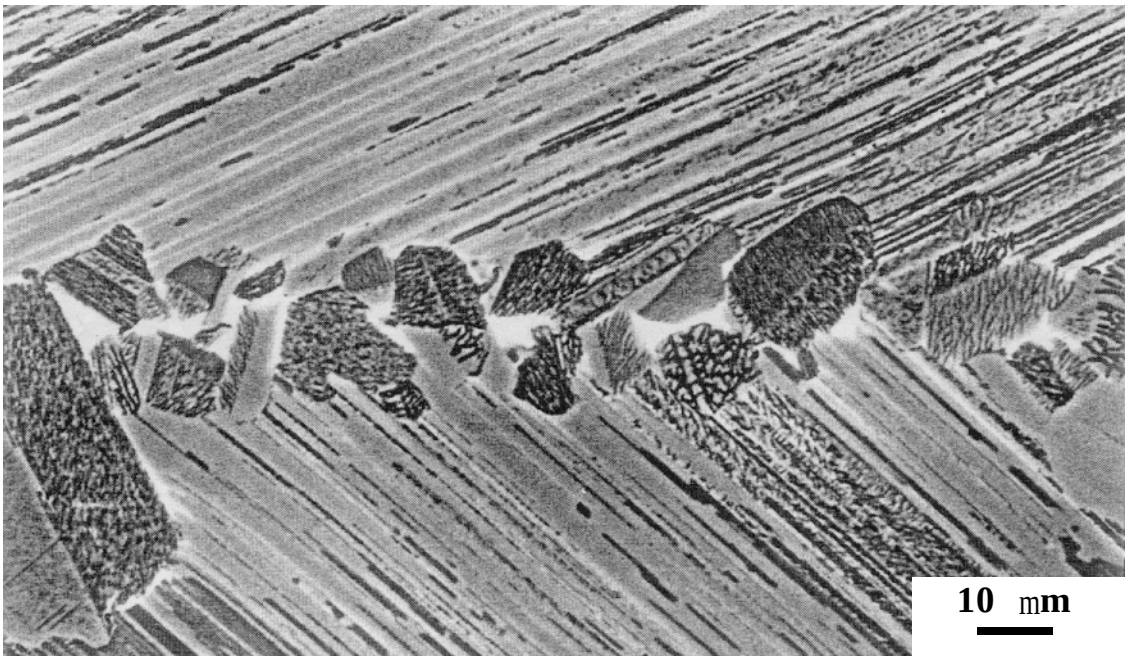

Figure 31. Weld line of diffusion welded cast Ti-48Al-2Mn-2Nb showing fine recrystallized grains [63].

cast and HIP'ed Ti-33Al-2Fe-1.8V-0.1B (wt%) alloy using hot-isostatic pressing. Cylindrical specimens ground with SiC down to 1200 grit, and chemically cleaned, were HIP'ed at temperatures of 900, 940 and 980^{o}C with a pressure of 200 MPa for one hour. IMI 834 specimens were only HIP'ed at the 900^{o}C temperature. High integrity, porosity-free welds were produced for both dissimilar-alloy combinations, with an increase in the bond width with an increase in HIP temperature. Tensile strength of the joints compared well with that of the titanium aluminide at room temperature, 300^{o}C and 600^{o}C, with fracture occurring either in the gamma TiAl or at the joint interface. Creep failure occurred at the weld interface due to the formation of porosity at the interface and their linkage to form a crack that propagated into the gamma titanium aluminide during the later stages of creep.

Krestler et al. [72] investigated the diffusion welding of a Ti-47Al-4(Nb,Mn,Cr,Si,B) sheet alloy produced via a powder metallurgy processing route for potential application in the manufacture of hollow gamma low pressure turbine blades. Welds were produced between 1.2 mm thick sheet in the duplex microstructural condition at 1000^{o}C for times of 5-8 hours and at loads of 5-20 MPa. The welding of surface ground sheets (1200 SiC paper) using parameters of 5 MPa pressure and a minimum time of 8 hours resulted in a defect-free interface characterized by very fine recrystallized gamma grains. As noted by previous investigators, this interfacial recrystallization is promoted by the deformation of asperity peaks on the sheet surfaces during welding. At higher pressures, identical weld quality was obtained for shorter weld times. It is of interest to note that welds produced on chemically-etched specimens using

comparable conditions, and at pressures up to 20 MPa, exhibited unbonded areas at the weld interface. Compression overlap shear tests performed at room temperature found optimized welds to fail predominantly in the base metal, confirming a high integrity weld interface. Postweld heat treatment of the welds at 1430^{o}C/30 minutes, which resulted in the formation of a nearly fully lamellar microstructure, increased the shear strength of all of the welds, with failure occurring exclusively in the base metal. The high temperature used for postweld heat treatment also promoted welding of the unbonded areas in welds produced on chemically cleaned surfaces, and the failure of these welds in the base metal.

Electron beam diffusion welding (EBDW) is a process that uses an electron beam to heat the interfaces of two abutting and compressively loaded workpieces. Through control of the electron beam focus, rastering pattern and traversing rate, the interface between the workpieces can be heated in a controlled manner to diffusion welding temperatures without melting the workpiece surfaces. Threadgill and Dance [73] applied the EBDW process to join Ti-52Al and Ti-48Al-2Cr-2Nb gamma titanium aluminides with and without a V interlayer. They observed a necklace of fine gamma grains along the weld interface for autogenous welds in Ti-52Al, but little such nucleation and growth in Ti-48Al-2Cr-2Nb. Further studies by Threadgill and co-workers [74] investigated the EBDW of a cast Ti-48Al-2Mn-2Nb alloy 5 mm in thickness. The nucleation and growth of fine gamma grains at the weld interface in this weld was comparable to that previously observed for conventional diffusion welds in this alloy. Consistent with the microstructure, hardness did not vary appreciably across the weld interface region. Work by Baeslack et al. [75] characterized the structure of defect-free EBDW welds produced at TWI on 5 mm thick Ti-48Al-2Cr-2Nb forgings. The relatively low temperatures and

forces experienced during welding promoted negligible change in the duplex microstructure across the weld interface region (Fig. 32). Consistent with the previous work of Threadgill and Dance [73], they did not observe the nucleation of grains at the weld interface in this alloy (Fig. 33). Overheating of the weld interface at the edge of the specimen promoted localized temperatures in the alpha phase field, and cooling to a fully lamellar microstructure. Hardness evaluation showed essentially no change across the weld interface, except at the specimen edge where the lamellar microstructure was somewhat harder than the duplex microstructure (Fig. 32). Fracture of three-point bend specimens occurred with less than 3% elastic + plastic strain but remote from the weld.

3.5 Diffusion Brazing/Transient Liquid Phase Welding

Yan and Wallach [61] examined the transient liquid phase (TLP) diffusion welding of Ti-48Al using several sputter-coated alloys, including low-melting point alloys Ti-24.5 at% Ni, Ti-43 at% Cu, and high melting point alloys V-49 at% Ni and Ti-38 at% Mn. TLP weld microstructures for the low melting point alloys produced at a welding temperature of about 1020^{o}C/30 minutes exhibited an isothermally-solidified alpha-two microstructure containing intermetallics particles. In contrast, the welds produced with high melting point alloys at 1250^{o}C/10 minutes solidified as alpha phase, with no intermetallics particles. They attribute the absence of brittle intermetallics phases to the higher welding temperatures and the higher diffusivities at temperature and decrease in stability of the intermetallic phases with an increase in temperature. As with the interlayer diffusion welds, postweld heat treatments were used to homogenize the weld interface and generate an optimized microstructure. However, in order to preclude remelting of the interface and corresponding void formation, especially for the low

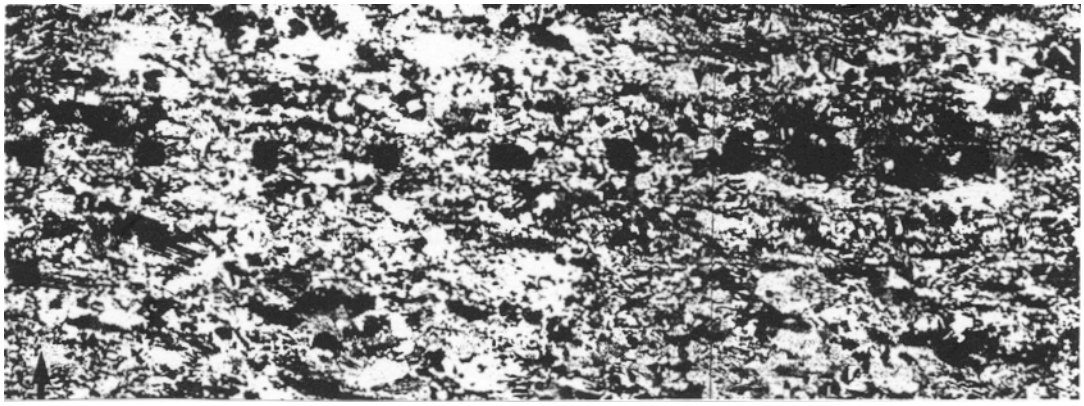

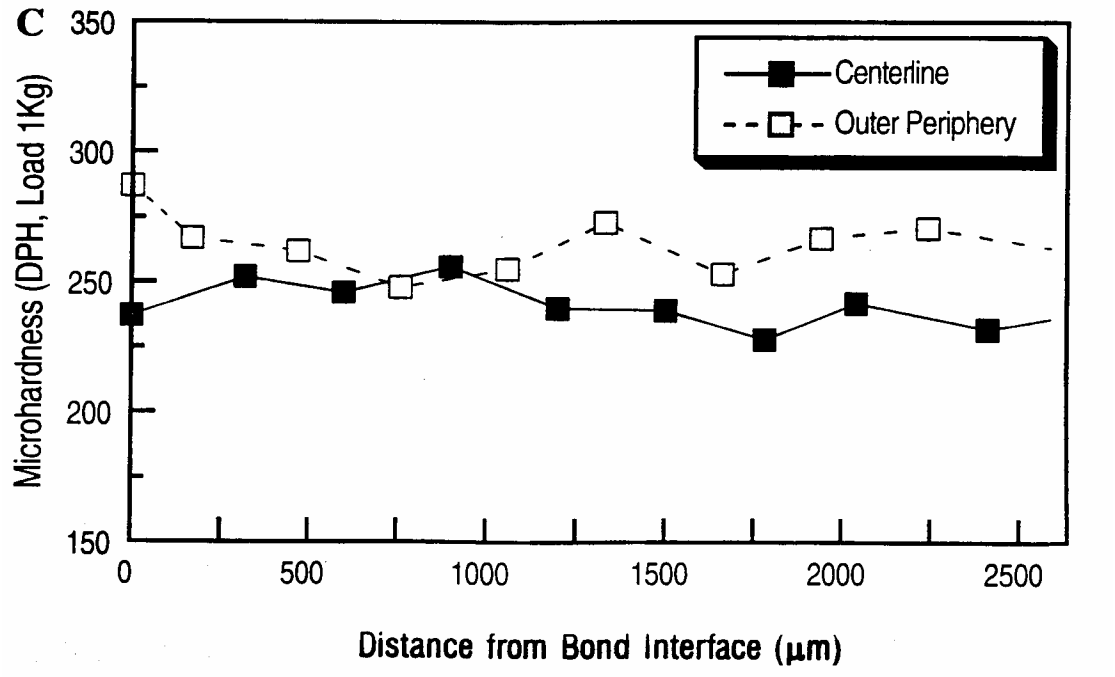

Figure 32. Light micrograph of electron beam diffusion weld in wrought Ti-48Al-2Cr-2Nb and corresponding diamond pyramid hardness traverse. Arrow indicates weld interface [74].

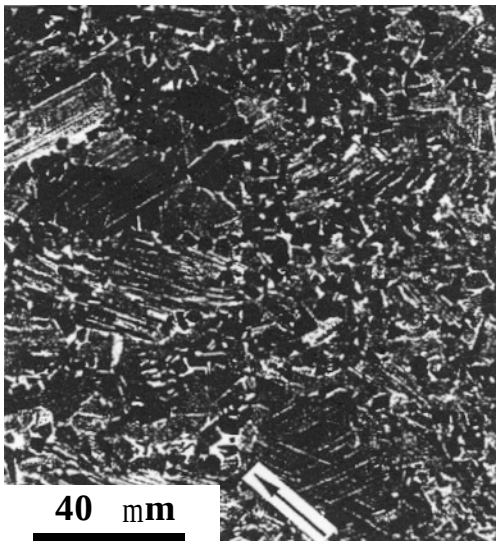

(a)

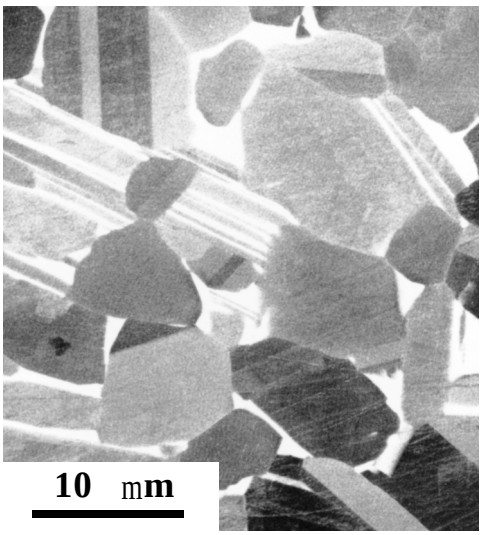

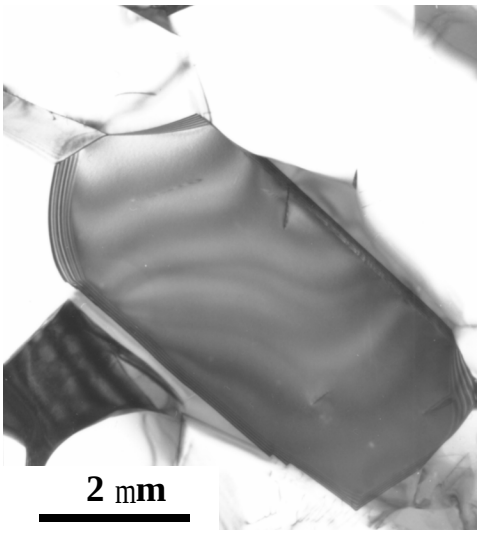

(b) (c)

Figure 33. SEM/BSE and TEM bright-field micrographs of electron beam diffusion weld interface (arrow) in Ti-48Al-2Cr-2Nb [74].

melting point alloy welds, a two-step heat treatment was developed. The first step involved a low temperature/long time heat treatment (eg. 1020^{o}C/40 hrs) designed to dissolve intermetallics particles, followed by a second high temperature treatment to homogenize the region and create an optimum microstructure (e.g., 1340^{o}C/40 minutes). Since intermetallics particles were not present in the high melting point filler metal welds, a single high temperature homogenization heat treatment was used to optimize the microstructure and mechanical properties. Final microstructures typically exhibited a lamellar microstructure after homogenization. Shear strengths of the Ti-Ni welds were poor following the low temperature homogenization, but increased significantly following the optimization heat treatment at high temperature. In contrast, excellent strength and ductility comparable to those of the parent material were obtained for the V-Ni filler alloy following high temperature heat treatment at 1340^{o}C, with failure occurring in the base metal.

Thakur et al. [76] investigated the transient liquid phase welding of a Ti-45Al-2Nb-2Mn-TiB_2 XD alloy using Al and Al/Ti/Al foil interlayers. Welds were produced using a range of foil thicknesses at a temperature of 900^{o}C and a pressure of 20 MPa for one hour. Analysis of the weld produced with Al foil showed the formation and cracking of an extremely hard and brittle $TiAl_3$ phase at the weld interface region. The alternate use of an Al/Ti/Al sandwich of foils minimized cracking problems, although appreciable $TiAl_3$ was formed during the welding process. It should be noted that this process is really a transient liquid phase versus a diffusion welding process, since the Al melts during the thermal cycle, and isothermally forms $TiAl_3$. Through appropriate control of the foil thicknesses, and the application of a long-term annealing treatment following

welding (1050°C/1 week) a crack-free weld zone microstructure comprised of gamma and alpha-two was achieved. Through proper control of the foil thickness to achieve a composition equal to that of the base metal, and the application of a high temperature homogenization heat treatment (1350°C/1 hr) after welding, the authors were able to achieve a lamellar gamma/alpha-two weld zone microstructure and a uniform composition across the joint comparable to that of the base metal.

Xu et al. [77] further investigated the feasibility of diffusion brazing Ti-45Al-2Nb-2Mn + 0.8 vol%TiB_2 XD alloy both to itself and to Ti-6Al-4V. They determined that the use of a Ti-15 wt%Cu-15 wt% Ni thin foil, or a Cu-Ni/Ti/Cu-Ni thin foil (5-10 microns) sandwich resulted in the production of high-integrity (i.e., excellent wetting, no porosity) bonds, whereas the use of a Cu-Ni foil was unsuccessful due to poor wetting. Joints were produced using a range of temperatures from 990-1100°C for between 5 and 30 minutes. Postbrazing heat treatments included a homogenization heat treatment between 1000 and 1100°C for two days to one week, and a subsequent heat treatment at 1310°C for 30 minutes. The as-brazed samples typically exhibited a large interdiffusion zone that contained a resolidified region comprised of large, elongated intermetallics directly at the bond centerline, surrounded by a constituent of alpha-two phase and fine intermetallic particles. The high hardness (over DPH 700) and brittleness of the intermetallics in the as-brazed joint resulted in poor bending strength. Postbraze heat treatment at temperatures of 1000 to 1200°C, which were below the liquation temperature of the bond, resulted in complete dissolution of the intermetallics particles, and a joint comprised of gamma, alpha-two and alpha phase. A further heat treatment at 1310°C/30 minutes was required to eliminate the alpha phase and optimize the bond region

microstructure. Mechanical testing of this fully-optimized joint revealed a hardness somewhat higher than that of the base metal (DPH 450 versus 350) and a bending strength comparable to that of the base material. The investigators also determined that high integrity joints between the gamma titanium aluminide and Ti-6Al-4V could be produced using the Cu-Ni alloy.

Das and Barone [78] investigated the diffusion brazing of a Ti-47Al-2Mn-2Nb-0.8vol% TiB_2 XD alloy to Ti-35V-15Cr (Alloy C) using Ti-27.5Cu-18.5Ni thin foils (25 and 70 microns in thickness). They observed that diffusion brazing at 1780°F/2hr achieved good quality bonds free of porosity, but a brittle joint microstructure comprised of alpha-two phase and a wide variety of Cu and Ni-rich intermetallics phases. They observed that the extent of the interdiffusion zone was much greater in the Alloy C than the titanium aluminide. Postbraze heat treatment at 971°C for 8 hr promoted further broadening of the interdiffusion zones, and the types of intermetallics phases changed. It is unclear from this analysis whether the braze region partially remelted during postbraze heat treatment. Hardnesses of the bond region for both the as-brazed and postbraze heat-treated conditions were appreciably greater than that of the gamma or Alloy C base materials. Room temperature three-point bending strength of the as-brazed joints was well below that of the base alloys. Postbraze heat treatment improved the bending strength but it was still only 60% that of the titanium aluminide. Fracture occurred along the bond/matrix interface in a brittle manner. Room and elevated-temperature (427°C) tensile strength of the bonds was well below that of the base metals, about 65% of the gamma alloy. As with the bend specimens, fracture occurred with negligible ductility at the bond line in a brittle manner. Although postbraze heat treatment had little beneficial

effect on tensile properties, the use of a thinner interlayer and a longer postbraze heat treatment time (12 hours) promoted joint efficiency of 81% and improved ductility. This improvement was attributed to a reduction in the level of intermetallics phases in the bond region.

Keisuke and co-workers [79] investigated the joining of TiAl using an Al filler metal via a self-propagating high temperature synthesis reaction. Joints produced using Al filler metal at 900^{o}C were comprised of $TiAl_3$ and $TiAl_2$. Postbraze heat treatment at 1300^{o}C promoted single-phase gamma in the joint and a strength comparable to that of the base metal. A subsequent investigation by these investigators [80] used a self-propagating high temperature synthesis reaction to produce a joint of $TiAl_3$ and Ti_3Al. Postweld heat treatment promoted a fine lamellar constituent in the joint, and room temperature strength comparable to that of the base metal.

Blue et al. [81] characterized microstructure evolution during the diffusion brazing of a forged Ti-48Al gamma titanium aluminide using a Ti-15wt%Cu-15wt%Ni thin foil 100 microns in thickness. Joints produced using infrared heating at 1150^{o}C for comparatively short brazing times ranging from 5 to 40 seconds exhibited excellent wetting between the braze alloy and the base metal, and contained no porosity. The width of the braze joints was quite similar to the thickness of the brazing foil, indicating minimal erosion of the substrate materials, which is consistent with the short braze times. As noted by other investigators, they observed coarse islands of Ti-Cu-Ni intermetallics at the center of the braze joint. Based on the ternary Ti-Cu-Al ternary phase diagram, they proposed that the surrounding matrix was comprised of alpha-two phase and beta titanium, which is consistent with more detailed characterization provided by other

investigators. Postbraze heat treatment at 900°C for 2 hours promoted dissolution of the coarse intermetallics.

Annaji and Lin [82] used the infrared brazing process to join Ti-48Al-2Nb-2Cr using a Ti (50 microns) and Al (60 microns) foil sandwich. Joining temperatures ranged from between 1200°C and 1275°C for times from 0 to 60 seconds. Postbrazing heat treatment of the joints was performed at temperatures between 1200°C and 1300°C for times between 1 and 4 hours. Joints in the as-brazed condition were characterized by voids and a large proportion of alpha-two martensite. Correspondingly, the joints exhibited poor mechanical properties. Postbraze heat treatment homogenized the composition and resulted in a lamellar alpha-two/gamma microstructure that exhibited higher strength and fracture outside of the joint region.

4. DISCUSSION OF FACTORS THAT CONTROL WELDABILITY AND PERFORMANCE

4.1 Solidification cracking

As with conventional titanium alloys, solidification cracking is generally not a problem in the fusion welding of gamma titanium aluminides. This can be attributed to the relatively narrow solidification range associated with the base ternary and quaternary compositions, such as Ti-48Al-2Nb-2Cr, and with the absence of alloying and/or impurity elements that promote the formation of low-melting eutectic phases. The only documented evidence of solidification cracking, by Lee [43], occurred in Ti-48Al-2Nb-2Cr at very high heat input weld that because of the weld geometry exhibited a high degree of solidification shrinkage stress at the weld centerline. The absence of solidification cracking in heavy section welds produced by Kelly [39] further confirms

the high intrinsic resistance of gamma titanium aluminide alloys to this problem. It is important to note that as alloy chemistries become more complex, particularly with the addition of minor alloying element that may partition more extensively during solidification, and thereby expand the solidification temperature range, susceptibility to solidification cracking may increase.

4.2 Solid-State Cracking

Solid-state cracking will continue to be problematic in both the fusion and solid-state joining of gamma titanium aluminides. In order to minimize the potential for this defect, one or both of the underlying mechanisms must be addressed through process control. First, the magnitude and distribution of thermal stresses developed during the welding process must be minimized through appropriate control of the weld heat sources (including the primary heating source such as an arc or high-energy beam and secondary sources such as quartz lamps or resistance heaters), component design, joint geometry, fixturing design, and postweld processing. Since it is difficult to minimize thermal stresses with a low energy input due to the high temperature gradients experienced, the production of crack-free fusion and solid-state welds will generally require the use of high energy inputs both from the primary energy source, and from supplemental heating sources, to minimize temperature gradients across the workpiece, cooling rates to room temperature, and correspondingly residual thermal stresses. The occurrence of stress raisers, such as the notch at the boundary between the fusion zone and the base metal, must also be minimized or eliminated.

In addition to a high stress, solid-state cracking requires a susceptible microstructure. Through control of alloy chemistry, and more importantly the weld

thermal cycle, it will be important to produce weld microstructures that exhibit optimum toughness and ductility. Based on work of several investigators, this means assuring a weld cooling rate that is sufficiently slow to minimize or eliminate the presence of retained alpha-two phase. In some instances, filler metal alloy chemistry may be modified to promote rapid alpha-two decomposition kinetics, although crack initiation and propagation in the weld HAZ could still be problematic.

Fortunately, both of the aforementioned requirements, reducing thermal stresses and promoting a fully-transformed microstructure, have been achieved through a high weld heat input and slow weld cooling rate. The effective use of many processes, in particular gas tungsten-arc, laser and electron beam welding of plate materials, will require the application of an external source of energy to provide suitable preheat, interpass and cooling rate control. This will mean additional complexity and expense of the joining process.

4.3 Microstructural Evolution and Control

Weld solidification behavior of gamma titanium aluminides influences the room temperature weld zone microstructure, including microstructures that have been postweld heat treated at high temperature. Generally, alloys with lower aluminum compositions tend toward a more columnar grain macrostructure, whereas alloys with higher Al contents solidify with a more equiaxed appearance. The orientation of the lamellar alpha-two + gamma constituent typical of the as-welded microstructure is directly influenced by the columnar grain orientation, and therefore by the solidification behavior. Postweld heat treatment studies on a variety of weld types have shown that even after appreciable recrystallization of the as-welded lamellar microstructure, the resulting duplex

microstructure exhibits a texture that can be attributed to the original solidification structure.

Continuous-cooling phase transformations and the resulting as-welded microstructure in the fusion zone and near-HAZ are a strong function of the weld cooling rate. High cooling rates associated with conventional EB and LB welding ($>10^3$ $^oC/s$) result in retention of the alpha phase and its ordering to alpha-two phase. Intermediate cooling rates achieved through preheating of the workpiece during EB and LB welding, or during GTA and friction welding, typically results in a massive or Widmanstatten gamma microstructure. At slower cooling rates obtained through preheat and process parameter control, a fully lamellar alpha-two + gamma constituent is obtained, with the coarseness of the constituent increasing with decreasing cooling rate. As shown in the previously described work of Godfrey et al. [39], it is not uncommon for the weld zone to contain a mixture of these various phases, particularly at intermediate cooling rates.

Postweld heat treatment at temperatures above 1000^oC promotes decomposition of metastable alpha phase, and recrystallization to a duplex structure comprised of equiaxed gamma and lamellar constituent. Unfortunately, a systematic study of PWHT effects on a range of initial weld microstructures, from fully retained alpha-two, to fully lamellar, has not been performed to date.

4.5 Microstructure/Mechanical Property/Fracture Relationships

The continuously-cooled weld zone microstructures described above are nearly always harder and stronger than the cast + HIP'ed + heat-treated, or forged + heat-treated base metal microstructures, and therefore the as-welded joint efficiency exceeds 100%. Postweld heat treatment produces softer fusion and near-HAZ microstructures, however,

the relatively fine nature of these microstructures versus the base metals retains their higher hardness and strength. Conversely, ductility of the finer, harder massive and Widmanstatten gamma transformation products, and of the fine lamellar microstructures, are typically well below that of the base metal. Postweld heat treatment at intermediate temperatures promotes recrystallization and coarsening of these microstructures with a corresponding improvement in ductility to levels approaching that of the base metal. Although the toughness of welds exhibiting alpha-two, massive, or Widmanstatten gamma microstructures have not been determined, work by Jensen et al. [40] has shown that the toughness of fine lamellar microstructures in Ti-48Al-2Nb-2Cr EB welds to be superior to those of the recrystallized microstructures produced through postweld heat treatment. Therefore, achieving the best combination of strength, ductility, and toughness will require an as-welded microstructure + postweld heat treatment that results in an appropriate microstructural balance of equiaxed gamma and lamellar alpha-two + gamma constituent.

5. CONCLUSIONS

Several broad conclusions can be drawn from this interpretive assessment and review of the state-of-the-art of joining gamma titanium aluminides:

1. Welding processes, process parameters and other welding conditions including preweld cleaning and atmospheric shielding requirements for the fusion welding of gamma titanium aluminides generally compare closely with those of conventional titanium alloys. However, welding systems must often provide additional capabilities to control and reduce the weld cooling rate in order to optimize the weld microstructure and thereby minimize weld cracking and

enhance weld mechanical properties. Solid-state welding processes commonly used to join conventional titanium alloys are likewise readily applicable to gamma titanium aluminides, although the substantially greater elevated-temperature strength of the gamma titanium aluminides versus conventional titanium alloys, and requirements for relatively slow weld cooling rates, typically demand different welding parameters.

2. The weldability of gamma titanium aluminides, simply defined as the ability to produce a high-integrity, defect-free weld joint exhibiting mechanical properties comparable to that of the base metal, is generally poorer than conventional titanium alloys. Although not susceptible to fusion zone solidification or HAZ liquation cracking, these alloys are highly susceptible to solid-state cracking during weld cooling that originates from the combination of brittle weld zone microstructures and high welding thermal stresses, and possibly environmental effects. Such cracking can be precluded if weld cooling rates are controlled such that a fully-transformed gamma + alpha-two microstructure is produced. Effective atmospheric protection both during and immediately subsequent to welding and postweld heat treatment immediately following welding further minimize the potential for this cracking problem.
3. Weld zone microstructures range from predominantly retained alpha-two phase and massive gamma, at the weld highest cooling rates, to mixtures of alpha-two phase, massive gamma, Widmanstatten gamma, and lamellar gamma + alpha-two phase for intermediate and slow weld cooling rates. As described previously, external preheat/interpass temperature control systems can markedly reduce the

weld cooling rate, leading to fully transformed, crack resistant microstructures. Postweld heat treatment can promote further transformation and recrystallization of these as-welded microstructures to duplex type microstructures comprised of equiaxed gamma grains and lamellar gamma + alpha-two constituent. Through a combination of weld cooling rate and postweld heat treatment temperature, weld microstructures can be controlled to optimize desired mechanical properties. For example, a weld cooled at an intermediate cooling rate may exhibit a fine Widmanstatten + lamellar microstructure that is both higher in strength than the base metal, and relatively tough. Alternatively, a weld cooled at a slow rate, followed by postweld heat treatment, could exhibit a recrystallized duplex microstructure that is more ductile than the aforementioned microstructure, but weaker and less tough. In the future, appreciable more work will be required to develop and optimize relationships between weld cooling rate, postweld heat treatment, microstructure and mechanical properties, particularly for second tier mechanical properties.

6. REFERENCES

1. DIMIDUK, D. M., "Gamma titanium aluminide alloys – an assessment within the competition of aerospace structural materials," Materials Science and Engineering, A263 (1999) 281.

2. C. M. AUSTIN, T. J. KELLY, K. G. MCALLISTER and J. C. CHESNUTT, "Aircraft engine applications for gamma titanium aluminides," Structural Intermetallics 1997, (M. V. Nathal, R. Darolia, C. T. Liu, P. L. Martin, D. B.

Miracle, R. Wagner and M. Yamaguchi, eds), TMS, Warrendale, PA (1997) 413-425.

3. P. A. BARTOLOTTA and D. L. KRAUSE, "Titanium aluminide applications in the high speed civil transport," Gamma Titanium Aluminides 1999, (Y. W. Kim, D. M. Dimiduk and M. H. Loretto, eds.) TMS, Warrendale, PA (1999) 3-10.
4. P. L. THREADGILL, "The prospects for joining titanium aluminides," Materials Science and Engineering A, 192/193 (1995) 640-646.
5. P. L. THREADGILL, CRP Report 463/1992, TWI, Cambridge (1992).
6. L. S. SMITH and P. L. THREADGILL, "The physical and welding metallurgy of titanium aluminides – a review," CRP Report 633/1998, TWI, Cambridge (1998).
7. G. CAM and M. KOCAK, "Progress in the joining of advanced materials," International Materials Reviews, 43 (1998) 1-45.
8. Y. W. KIM, "Trends in the development of gamma TiAl Alloys," Gamma Titanium Aluminides (Y. W. Kim, R. Wagner and M. Yamaguchi, eds.) TMS, Warrendale, PA (1995) 637-654.
9. C. MCCULLOUGH, J. J. VALENCIA, C. G. LEVI AND R. MEHRABIAN, "Phase equilibria and solidification of Ti-Al Alloys," Acta Met. 37 (1989) 1321-1336.
10. J. J. VALENCIA, C. MCCULLOUGH, C. G. LEVI AND R. MERHABIAN, "Solidification microstructure of supercooled Ti-Al alloys containing intermetallic phases," Acta Met. 37 (1989) 2517-2530.
11. K. MURALEEDHARAN, L. L. RICHEL, M. DE GRAER, A. W. CRAMB, T. M. POLLOCK AND G. T. GRAY III, "The effect of cooling rate during casting

on microstructural development in Ti-48Al-2Cr-2Nb type alloys," Structural Intermetallics (M. Nathal, R. Darolia, C. Liu, P. Martin, D. Miracle, R. Wagner and M. Yamaguchi, eds.), TMS. Warrendale, PA (1997) 215-224.

12. M. DE GRAEF, N. BIERY, L. RICHEL, T. M. POLLOCK AND A. CRAMB, "On the relation between cooling rate and solidification microstructure in as-cast titanium aluminides," Gamma Titanium Aluminides 1999 (Y. W. Kim, D. M. Dimiduk and M. H. Loretto, eds.) TMS, Warrendale, PA (1999) 247-254.

13. D. M. DIMIDUK AND V. K. VASUDEVAN, "Isothermal and continuous cooling decomposition of alpha and beta phases in gamma titanium aluminides," Gamma Titanium Aluminides 1999 (Y. W. Kim, D. M. Dimiduk and M. H. Loretto, eds.) TMS, Warrendale, PA (1999) 239-246.

14. P. WANG AND V. K. VASUDEVAN, "Composition dependence of the massive transformation from alpha to gamma in quenched TiAl alloys," Scripta Met. et Mat., 27 (1992) 89-94.

15. G. RAMANATH AND V. K. VASUDEVAN, "The alpha to gamma transformation during continuous cooling in Ti-48 at% Al alloys," Mat. Res. Soc. Symp., 288, MRS (1993) 223-228.

16. P. WANG and V. K. VASUDEVAN, "Effect of cooling rate on decomposition of the alpha phase in Ti-(43-50) at% Al alloys," Mat. Res. Soc. Symp., 288, MRS (1993) 229-236.

17. M. TAKEYAMA, T. KUMAGAI, M. NAKAMURA AND M. KIKUCHI, "Cooling rate dependence of the alpha/gamma phase transformation in titanium aluminides and its application to alloy development," Structural Intermetallics,

(R. Darolia, J. J. Lewandowski, C. T. Liu, P. L. Martin, D. B. Miracle and M. V. Nathal, eds.), TMS, Warrendale, PA (1993) 167-176.

18. T. KUMAGAI, E. ABE, AND M. NAKAMURA, "Microstructure evolution through the alpha to gamma phase transformation in a Ti-48 at. pct. Al alloy," Met and Mat. Trans. A, 29A (1998) 19-26.

19. T. J. KELLY, "Repair welding of gamma titanium aluminide castings," Proc. 3rd International SAMPE Metals Conference, Covina, CA (1992) 183-191.

20. L. C. MALLORY, W. A. BAESLACK III, D. PHILLIPS and T. J. KELLY: "Gas tungsten-arc welding of a Ti-48Al-2Cr-2Nb gamma titanium aluminide," Titanium 92 Science and Technology, (F. H. Froes and I. Caplan, eds.), TMS, Warrendale, PA (1993) 1115-1122.

21. L. C. MALLORY, W. A. BAESLACK III, and D. PHILLIPS, "Evolution of the weld HAZ microstructure in a Ti-48Al-2Cr-2Nb gamma titanium aluminide," Journal of Materials Science Letters, 13 (1994) 1061-1065.

22. Y. W. KIM and D. M. DIMIDUK, "Progress in the understanding of gamma titanium aluminides," Journal of Metals, 43 (1991) 40-47.

23. P. L. THREADGILL and B. G. I. DANCE, "Joining of intermetallic alloys; further studies," TWI Members Report 498, TWI, Cambridge (1994).

24. S. HURTA, H. CLEMENS, G. FROMMEYER, H. P. NICOLAI, H. SIBUM, "Valves of intermetallic gamma-TiAl-based alloys: processing and properties," Titanium '95: Science and Technology, (P. A. Blenkinsop, W. J. Evans and H. M. Flower, eds.) Institute of Materials, London (1996) 277-286.

25. V. L. ACOFF and D. J. BHARANI, "Effect of weld heat input on fusion zone morphology of gamma TiAl," Proceedings from Materials Solutions '97 on Joining and Repair of Gas Turbine Components, Indianapolis, IN, ASM International, Materials Park, OH (1997) 137-142.

26. D. J. BHARANI and V. L. ACOFF, "Autogenous gas tungsten-arc weldability of cast alloy Ti-48Al-2Cr-2Nb (at%) versus extruded alloy Ti-46Al-2Cr-2Nb-0.9Mo (at%)," Met. Trans. A., 29A (1997) 927-935.

27. V. L. ACOFF and M. ARENAS, "Evolution of the fusion zone microstructure using autogenous gas tungsten arc welding of gamma titanium aluminide," Proceedings from Materials Conference '98 on Joining of Advanced and Specialty Materials, (M. Singh J. E. Indacochea and D. Hauser, eds.) Rosemont, IL, ASM International, Materials Park, OH (1998) 101-105.

28. M. ARENAS, S. AGEE, V. L. ACOFF, "Autogenous gas tungsten arc welding of gamma titanium aluminide and the effects of postweld heat treatment," Gamma Titanium Aluminides 1999, (Y. W. Kim, D. M. Dimiduk and M. H. Loretto, eds.), TMS, Warrendale, PA (1999) 335-340.

29. Q. XU, M. C. CHATURVETI, N. L. RICHARDS, "Evaluation of gas tungsten-arc welding of a Ti-45Al-2Nb-2Mn + 0.8TiB_2 alloy," Trends in International Welding Research, (J. Vitak, et al., eds.) ASM International, Materials Park, OH (1999) 245-250.

30. C. M. JENSEN, H. ZHANG, W. A. BAESLACK III, T. J. KELLY, "Effect of heat treatment on the structure of gas tungsten-arc welded Ti-48Al-2Cr-2Nb

titanium aluminide," presented at 1997 AWS National Meeting submitted for publication in Science and Technology of Welding and Joining.

31. J. BREEDING, J. C. LIPPOLD and W. A. BAESLACK III, "Postweld heat treatment of gas tungsten-arc welds in Ti-48Al-2Cr-2Nb titanium aluminides," to be published.

32. J. BREEDING, J. C. LIPPOLD and W. A. BAESLACK III, "Flux-assisted GTA Welding of Ti-48Al-Nb-2Cr titanium aluminide," Extended Abstract from AWS National Meeting, Cleveland, (2001).

33. R. A. PATTERSON, P. L. MARTIN, B. K. DAMKROGER and L. CHRISTODOLOU, "Titanium aluminide: electron beam weldability," Welding Journal, Research Supplement, (1990) 39s-44s.

34. R. A. PATTERSON and B. K. DAMKROGER, "Weldability of gamma titanium aluminide," Weldability of Materials, (R. A. Patterson and K. W. Mahin, eds.), ASM International, Materials Park, OH (1991) 259-267.

35. Y. W. KIM, "Intermetallic compound alloys based on gamma titanium aluminide," Journal of Metals, 41 (1989) 24-30.

36. S. P. GODFREY, P. L. THREADGILL, and M. STRANGWOOD, "Microstructural development during electron beam welding of Ti-48Al-2Mn-2Nb (at%)," 4th European Conference on Advanced Materials and Processes (Euromat 95), Venice (1995).

37. M. C. CHATURVEDI, N. L. RICHARDS and Q. XU, "Electron beam welding of a Ti-45Al-2Nb-2Mn + 0.8 vol% TiB2 XD alloy," Materials Science and Engineering, A239-240 (1997) 605-612.

38. Q XU, M. C. CHATURVEDI and N. L. RICHARDS, "The role of phase transformation in electron beam welding of TiAl-based alloys," Metallurgical and Materials Transactions A, 30A (1999) 1717-1726.

39. T. J. KELLY, "Electron beam welding of cast gamma titanium aluminides," Unpublished Report, GE Aircraft Engines, Evandale, OH (1998).

40. C. M. JENSEN, H. ZHANG, W. A. BAESLACK III, T. J. KELLY, "Effects of postweld heat treatment on the structure and properties of electron beam welded Ti-48Al-2Cr-2Nb (at%)," presented at 79th AWS Annual Meeting (1998). Submitted for publication in the Welding Journal Research Supplement.

41. W. A. BAESLACK III and P. L. THREADGILL, Unpublished work, TWI, Cambridge (1991).

42. T. SHINODA, K. ITO and C. HAYASHI, "Friction welding of TiAl intermetallic compound," Journal of Japanese Friction Welding Association, 3 (1996) 25-31.

43. J. LEE, "Laser Welding of Gamma Titanium Aluminides," Ph.D. Dissertation, The Ohio State University, Columbus, OH (1995).

44. J. LEE and W. A. BAESLACK III, "Laser welding of gamma titanium aluminides," Extended Abstract from AWS National Meeting, to be published in the Welding Journal Research Supplement.

45. M. KILASSEN, E. SHUBERT AND G. SEPOLD, "Laser Treatment of Materials" Arbeitgemeinshft Warmebehandlung and Werkstofftechnik (1996) 193.

46. H. CLEMENS et al., "Spacecraft, Structures, Materials and Mechanical Testing," Noordewijk, The Netherlands: European Space Agency, SP-386 (1996) 1297.

47. L. MALLORY, "HAZ phenomena in cast Ti-48Al-2Nb-2Cr and two modified alloys," Ph.D. Dissertation, The Ohio State University, Columbus, OH (1996).

48. K. N. HOU, M. C. JUHAS, W. A. BAESLACK III, H. L. FRASER, D. PHILLIPS: "An electron microscopy study of inertia-friction welds in Ti-48Al-2Cr-2Nb gamma titanium aluminide," Proceedings of International Conference on Trends in Welding Research, (J. Vitek et al., eds.), Gatlinburg, TN, ASM International, Materials Park, OH (1992) 1135-1137.

49. C. L. ENGLISH: "A study of the inertia weldability of a wrought gamma titanium aluminide," Master's Thesis, University of Cincinnati, Cincinnati, OH (1993).

50. H. ZHANG, C. M. JENSEN, T. J. KELLY, C. ENGLISH, W. A. BAESLACK III: "Microstructure Evolution During Postweld Heat Treatment of Inertia-Friction Welds in Ti-48Al-2Cr-2Nb (at%) Titanium Aluminide," to be published in Materials Characterization.

51. HORN, H., Investigations of friction welding titanium aluminides, Proc. Eurojoin I, Strasbourg (1991).

52. BAESLACK, W. A. III and THREADGILL, P. L., Unpublished research, TWI, Cambridge, UK (1990).

53. S. P. GODFREY, M. STRANGWOOD and P. L. THREADGILL, "Linear friction welding of a gamma titanium aluminide alloy," in Proceedings of SF2M Autumn Conference, Paris (1996).

54. BAESLACK, W. A. III, THREADGILL, P. L., NICHOLAS, E. D., and BRODERICK, T. F., "Linear friction welding of Ti-48Al-2Cr-2Nb (at%) titanium

aluminide," Titanium 95: Science and Technology, (P. A. Blenkinsop, W. J. Evans and H. M. Flower, eds.), The Institute of Metals, London (1995) 424-431.

55. T. J. LIENERT, K. JATA, V. SEETHARAMAN and R. T. WHEELER, "Friction stir welding of Ti-6Al-4V alloys," Proceedings of Conference on Joining of Advanced Specialty Materials III, ASM International, Materials Park, OH (2000).

56. M. C. JUHAS, G. B. VISWANATHAN and H. L. FRASER, "Characterization of microstructural evolution in a Ti-6Al-4V friction-stir weld," to be published.

57. Y. NAKAO, K. SHINOZAKI and M. HAMADA, "Diffusion bonding of intermetallic compound TiAl," ISIJ International, 31, (1991) 1260-1266.

58. Y. NAKAO, K. SHINOZAKI and M. HAMADA, "Diffusion bonding of intermetallic compound TiAl, International Trends in Welding Science and Technology (S. A. David and J. M. Vitek, eds.) , ASM International (1992) 1057-1061.

59. P. YAN, C. A. HIPPSLEY, M. STRANGWOOD and E. R. WALLACH, "Diffusion bonding titanium aluminide TiAl," Proceedings of International Conference on High Temperature Intermetallics, Royal Society, London, (1991) 184-187.

60. P. YAN, R. E. SOMEKH and E. R. WALLACH, "Solid-state bonding of TiAl with interlayers," International Trends in Welding Research, (S. A. David and J. M. Vitek, eds.), ASM International, Materials Park, OH (1992) 1063-1067.

61. P. YAN and E. R. WALLACH, "Diffusion-bonding of TiAl," Intermetallics, 1, (1993) 83-87.

62. S. P. GODFREY, P. L. THREADGILL and M. STRANGWOOD, “High temperature phase transformation kinetics and their effects on diffusion bonding of Ti-48Al-2Mn-2Nb,” in Proceedings of Euromat 2, Paris (1993).

63. S. P. GODFREY, P. L. THREADGILL and M. STRANGWOOD, “High temperature phase transformation kinetics and their effects on diffusion bonding of Ti-48Al-2Mn-2Nb,” Journal De Physique IV, Colloque C7, supplement to Journal De Physique III, Volume 3 (1993) 485-488.

64. S. P. GODFREY, P. L. THREADGILL and M. STRANGWOOD, “Diffusion bonding of Ti-48Al-2Mn-2Nb,” Proceedings of Symposium on High Temperature Ordered Intermetallic Alloys VI, MRS (1994).

65. G. CAM, K. H. BOHM, J. MULLAUER and M. KOCAK, “The fracture behavior of diffusion-bonded duplex gamma TiAl,” Journal of Metals 11 (1996) 66-68.

66. G. CAM, J. MLLAUER and M. KOCAK, Science and Technology of Welding and Joining, 2 (1997) 213-219.

67. K. H. BOHM, V. VENTZKE, G. CAM and M. KOCAK, Schweissen and Schneiden, 49 (1997) 660-671.

68. W.GLATZ and H. CLEMENS, “Diffusion bonding of Ti-47Al-2Cr-0.2Si sheet material,” Intermetallics, 5 (1997) 415-423.

69. M. HOLMQUIST, “Hot isostatic diffusion bonding of titanium alloy Ti-6Al-4V to gamma titanium aluminide IHI alloy 01A,” Scripta Materialia, 39 (1998) 1101-1106.

70. M. HOLMQUIST, V. RECINA and B. PETTERSSON, "Tensile and creep properties of diffusion bonded Alloy IMI834 to gamma titanium aluminide IHI alloy 01A," Acta Materilia, to be published.

71. M. HOLLMQUIST, V. RECINA and B. PETTERSSON, "Tensile and creep properties of diffusion bonds between two titanium alloys and a gamma titanium aluminide," Gamma Titanium Aluminides 1999, (Y-W. Kim, D. M. Dimiduk and M. H. Loretto, eds.), TMS, Warrendale, PA (1999) 431-438.

72. H. KESTLER, H. CLEMENS, H. BAUR, R. JOOS, R. GERLING, G. CAM, A. BARTELS, C. SCHLEINZER AND W. SMARSLY, "Characterization of Gamma-TiAl Sheet Material for Aeroengine Application," Gamma Titanium Aluminides 1999, (Y-W Kim, D. M. Dimiduk and M. H. Loretto, eds.), TMS, Warrendale, PA (1999) 423-430.

73. P. L. THREADGILL and B. G. I. DANCE, "Joining of intermetallics alloys; further studies, TWI Members Report 498, TWI, Cambridge (1994).

74 P. L. THREADGILL, "Further progress in the joining of intermetallics alloys," TWI Members Report, 536/1995, TWI, Cambridge (1995).

75 .W. A. BAESLACK III, H. ZHENG, P. L. THREADGILL, B. G. I. DANCE, "Characterization of an electron beam diffusion bond in Ti-48Al-2Cr-2Nb Titanium Aluminide," Materials Characterization, 39 (1997) 43-52.

76. Q. THAKUR, Q. XU, M. C. CHATURVEDI, N. L. RICHARDS, N. GOEL, "Diffusion bonding of a TiAl Alloy with Al and Al/Ti/Al Interlayers," Trends in Welding Research, (J. Vitek et al., eds.) ASM International, Metals Park (1999) 635-640

77. Q. XU, M. C. CHATURVEDI, N. L. RICHARDS and N. GOEL, Diffusion brazing of a Ti-45Al-2Nb-2Mn-0.8vol% TiB2 XD alloy, Structural Intermetallics, (M. V. Nathal, R. Darolia, C. T. Liu, P. L. Martin, D. B. Miracle, R. Wagner and M. Yamaguchi, eds.), TMS, Warrendale, PA (1997) 323-329.

78. G. DAS and C. BARONE, "A study of diffusion bonding of dissimilar titanium alloys," Unpublished research.

79. U. KEISUKE, S. HIROYUKI, F. KIJIRO, "Joining of intermetallics compound TiAl using Al filler material," Z. Fur metalKunde, 86 (1994) 270-274.

80. U. KEISUKE, S. HIOYUKI, F. KIJIRO, "Joining of intermetallics compound TiAl using self-propagating high temperature synthesis reaction," Zeitschrift Fur Metalkund, V86 (1995) 64-68.

81. C. A. BLUE, R. A. BLUE and R. Y. LIN, "Microstructural evolution in joining of TiAl with a liquid Ti Alloy," Scripta Metallurgica et Materialia, 32 (1995) 127-132.

82. S. ANNAJI and R. Y. LIN, "Infrared brazing of a TiAl-base alloy using Ti and Al foils and the joint microstructural evolution," Structural Intermetallics 1997, (M. V. Nathal, R. Darolia, C.T. Liu, P L. Martin, D. B. Miracle, R. Wagner and M. Yamaguchi, eds.), TMS, Warrendale, PA (1997) 395-404.